Field metabolic rates of Scotia Sea myctophids (family Myctophidae)

Confirmation Report

Sarah R. Alewijnse

August 9, 2019

Contents

1 Abstract

Myctophids (family Myctophidae) are an important part of the biological carbon pump in the oceans. Estimating the magnitude of their contribution to the biological carbon pump requires knowledge of their field metabolic rate; the time-averaged rate at which they use energy while free-ranging in their natural environment. Here, I present the first estimates of relative field metabolic rate for six species of myctophids (*Electrona antarctica, E. carlsbergi, Gymnoscopelus braueri, G. nicholsi, Protomyctophum bolini* and *Krefftichthys anderssoni*) from the Scotia Sea, using a novel proxy for field metabolic rate based on otolith δ^{13}C. Contrary to metabolic theory, differences among species were the most important drivers of variation in metabolic rate, rather log body mass and temperature. I explore why field metabolic rate is different among these species by comparing the ecology and life history characteristics of the six species. Additionally, estimates of field metabolic rate did not positively correlate with estimates of resting metabolic rate, suggesting that current calcuations of myctophid contribution to the biological carbon pump in the Scotia Sea are inaccurate.

2 Introduction

Mesopelagic fishes (those living in the mesopelagic zone, between 150-1000m) are an important component of the ocean biological carbon pump (Anderson et al., 2018; Trueman et al., 2014). They oftern undertake diel vertical migrations, swimming from depth to surface waters at night to feed on zooplankton, before returning to the deep prior to daybreak. By completing this diel vertical migration, migratory mesopelagic fishes transport carbon away from the surface waters, and export this carbon in the mesopelagic through respiration, excretion and mortality. Non-migratory mesopelagic fishes also contribute to the biological carbon pump by consuming migrating zooplankton in the mesopelagic zone (Davison et al., 2013). The deeper carbon is transported in the ocean, the longer it is prevented from returing to the surface and fluxing with the atmosphere (Passow and Carlson, 2012). Interest in harvesting mesopelagic fishes is increasing, driven by a growing requirement for fishmeal to sustain aquaculture (Catul et al., 2011; Davison et al., 2013; St. John et al., 2016). To fully understand the potential impact of harvesting mesopelagic fishes, we must first quantify the role they play in the biological carbon pump.

Myctophids (family Myctophidae) are the dominant mesopelagic fishes in the Scotia Sea, a highly productive area of the Southern Ocean. (Catul et al., 2011; Collins et al., 2012). Scotia Sea myctophids are estimated to contribute 0.05 to 0.28 mg C m^{-2} d^{-1} to active carbon flux, equivalent to 9 to 47% of gravitational particulate organic carbon flux in the same area (Belcher et al., 2019). This estimate is obtained by estimating myctophid metabolic rate from the regression equation:

$$Ln(RMR_W) = a + b_W \times Ln(WM) + b_T \times T \tag{1}$$

Where RMR_W is wet mass-specific resting metabolic rate (µl O_2 mg WM^{-1} h^{-1}), and T is temperature (°C).

This equation was parameterised based on five studies of myctophid respi-

ration rate, (Ariza et al., 2015; Donnelly and Torres, 1988; Ikeda, 1989; Torres and Somero, 1988a; Torres et al., 1979) measured through either respirometry or electron transport system enzyme activity (ETS), both of which are less than ideal methods for this group of fishes. Myctophids are delicate fishes, and are often dead or damaged on landing (Catul et al., 2011). Consequently, fishes which are subjected to respirometry are likely to be stressed, giving artificially high measures of metabolic rate. These studies selected the most active fish in a catch, which potentially biases measures towards fish with higher metabolic rates (Torres and Somero, 1988a). ETS measures the respiration potential of a sample of tissue, which is then converted to whole organism metabolic rate using a ratio of ETS and respirometry (Ariza et al., 2015; Cammen et al., 1990; Ikeda, 1989). No direct calibrations between ETS and oxygen consumption are available for myctophids, which may lead to inaccurate estimates of metabolic rate.

Both of these methods measure or estimate resting metabolic rate (RMR), the minimum metabolic rate of a resting organism, in a post-absorptive state (Treberg et al., 2016). RMR is a less useful measurement of metabolic rate in the context of the biological carbon pump than field metabolic rate (FMR). FMR is the time-averaged energy expenditure of an organism free-ranging in its natural habitat (Treberg et al., 2016). FMR includes energy expended on basal costs, as with RMR, but also incorporates the thermic effect of food (also called specific dynamic action), as well as energy used for growth, reproduction, movement and excretion (Chung et al., 2019a,b; Treberg et al., 2016).

In this study I used a novel method to calculate M value, a proxy for mass-specific FMR (Chung et al., 2019a). Otoliths are calcium carbonate structures found in the inner ears of fishes. The carbon in the otolith comes from the surrounding endolymph, which itself comes from carbon in the blood (Campana, 1999; Solomon et al., 2006). Blood carbon comes from two sources: metabolic (dietary) carbon, produced during cellular respiration, and dissolved inorganic carbon from the surrounding water. These two sources of carbon are isotopically distinct, with dissolved inorganic

carbon having a greater proportion of carbon-13 to carbon-12, than metabolic carbon (δ^{13}C of dissolved inorganic carbon is 15‰ more positive δ^{13}C of metabolic carbon) (Magozzi et al., 2017; Tagliabue and Bopp, 2008). Fish with relatively higher metabolic rates have higher respiration rates, so produce more metabolic carbon. As fish regulate the levels of carbonate in their blood, this increase in metabolic carbon is compensated by a decrease in dissolved inorganic carbon, increasing the proportion of metabolic carbon in the blood, meaning (δ^{13}C) in the blood has a more negative value. Therefore δ^{13}C values of otoliths are a weighted average of δ^{13}C values from metabolic carbon and dissolved inorganic carbon (Chung et al., 2019a; Trueman et al., 2016). If δ^{13}C values are known, the proportion of metabolic carbon (M value) can be calculated, as was done in this study (section 3.1.2). While this is a novel method, a recent study confirmed that M values and oxygen consumption were positively correlated in cod (*Gadus morhua*), giving empirical support for the use of M as a metabolic proxy (Chung et al., 2019b).

The primary aim of this study is to use M values to compare relative FMR between six species of myctophids common in the Scotia Sea: *Electrona antarctica, E. carlsbergi, Gymnoscopelus braueri, G. nicholsi, Protomyctophum bolini* and *Krefftichthys anderssoni* (Collins et al., 2008, 2012; Piatkowski et al., 1994). This study is the first comparison of FMR between species of myctophids to date.

I will also investigate the scaling relationships of M values with body mass and temperature. According to the metabolic theory of ecology, metabolic rates scale linearly with log body mass and temperature (Brown et al., 2004). I will examine whether this is the case for FMR by modelling M values as a linear function of log body mass and temperature. If the metabolic theory is correct, M values should decrease with increasing log body mass, and increase with increasing temperature, both within and between species. Temperature is obtained from otolith stable isotopes, using δ^{18}O (section 3.1.3).

Finally, I will compare estimates of mass-specific RMR generated using equation 1, and M values. As RMR is likely to be a component of FMR, studies predict

that these two measures of metabolic rate will be positively correlated.

3 Methods

3.1 Data Collection

3.1.1 Otolith Stable Isotope Analysis

Otoliths from six species of myctophids from the Scotia Sea were donated by the British Antarctic Survey for this study: *Electrona antarctica* (n = 19), *E. carlsbergi* (n = 17), *Gymnoscopelus braueri* (n = 20), *G. nicholsi* (n = 13), *Krefftichthys anderssoni* (n = 20) and *Protomyctophum bolini* (n = 20). Due to a labelling error, eight *E. carlsbergi* individuals did not have body mass recorded, and were omitted for all body mass analyses.

Prior to stable isotope analysis, each otolith was cleaned in water, allowed to dry and mounted onto a backing plate (Struers EpoFix resin). The outer surface of the otolith (100-200 µm depth) was milled using an ESI NewWave Micromill, to ensure that the otolith material deposited most closely to the time of capture was analysed. Where the otoliths were too small to be milled (<1mm diameter - all *K. anderssoni* and some *P. bolini*), they were crushed to obtain powder for stable isotope analysis. Supplementary analyses (appendix C) were run to test whether this caused a significant difference in M values.

3.1.2 M Values

A mixing model was used to estimate the proportion of metabolic carbon in the blood, M:

$$M = \frac{\delta^{13}C_{oto} - \delta^{13}C_{DIC-SW}}{\delta^{13}C_{diet} - \delta^{13}C_{DIC-SW}} + e_{total} \tag{2}$$

Where $\delta^{13}C_{oto}$ is the δ^{13}C value of the fish's otolith, $\delta^{13}C_{DIC-SW}$ is the value for δ^{13}C of dissolved inorganic carbon (DIC) ingested by the fish through seawater, $\delta^{13}C_{diet}$

is the δ^{13}C of the diet, and e_{total} is the isotopic fractionation from DIC to blood, blood to endolymph, and endolymph to otolith. For this study I assumed that e_{total} was invariant across species, and that M values were directly proportional to the percentage of metabolic carbon in the fish's blood (Chung et al., 2019a).

In calculating M values, parameters were allowed to vary across normal and truncated normal (Mersmann et al., 2018) distributions with means, standard deviations, and minimum and maximum values set according to the relevant literature (appendix A). $\delta^{13}C_{DIC-SW}$ was set using catch location and corrected for the Suess effect (the decrease in δ^{13}C with time, due to anthropogenic carbon dioxide emissions), from the model by Tagliabue and Bopp (2008). $\delta^{13}C_{diet}$ was set using δ^{13}C of phytoplankton (set by catch location) from the model by Magozzi et al. (2017), trophic levels from Froese and Pauly (2019) and the trophic enrichment factor for carbon from DeNiro and Epstein (1978). e_{total} was set to the value from Solomon et al. (2006). 10,000 random samples were taken from the resulting distribution of M values for each individual.

3.1.3 Reconstructed Temperature

δ^{18}O of otolith aragonite can be used to estimate the ambient temperature experienced by a fish (Høie et al., 2004; Thorrold et al., 1997). Experienced temperature (T) was reconstructed using the following equation:

$$T = \frac{(\delta^{18}O_{oto} - \delta^{18}O_{SW}) - a}{b} \tag{3}$$

Where $\delta^{18}O_{oto}$ is the δ^{18}O of the otolith, $\delta^{18}O_{SW}$ is the δ^{18}O of the ambient seawater, and a and b are parameters, set according to Høie et al. (2004). $\delta^{18}O_{SW}$ was set according to Schmidt et al. (1999), by catch location and depth. As with M values, all parameters were allowed to vary across normal and truncated normal distributions (appendix B).

3.1.4 Estimates of log Mass-Specific Resting Metabolic Rate

Estimates of log specific resting metabolic rate (RMR) were calculated using equation 1. Parameters were set according to Belcher et al. (2019) so that a = -1.315($\pm$0.468), b_W = -0.2665 ($\pm$0.0516), and b_T = 0.0848($\pm$0.0108).

3.2 Statistical Analyses

All statistical analyses were carried out in R (R Core Team, 2018). Hamiltonian Monte Carlo (HMC) models were run in RStan (Stan Development Team, 2018) using the rethinking package (McElreath, 2016). Convergence and mixing were checked using effective sample size (N_eff), $\hat{\text{R}}$, and traceplots (appendix D).

To examine the effect of log body mass and temperature on M values, I modelled estimates of M values as a linear function of log body mass (W) and temperature (T) in an HMC simulation of 1,000,000 iterations, with 500,000 warmup, a single chain, and a thinning parameter of 1. Species was included in the model as a random factor to address the problem of pseudoreplication within species. This also gave estimates of the mean M value for each species, and allowed me to assess whether M values varied significantly between species.

Model 1 - Body Mass and Temperature

$$M_{est,i} \sim Normal(\mu_i, \sigma)$$

$$\mu_i = a_1 + b_W \times W + b_T \times T_{est,i} + a\_Var_{Species}$$

$$M_{obs,i} \sim Normal(M_{est,i}, M_{sd,i})$$

$$T_{obs,i} \sim Normal(T_{est,i}, T_{sd,i})$$

$$a_1 \sim Normal(0.20, 0.5)$$

$$b_W \sim Normal(0, 0.5)$$

$$b_T \sim Normal(0, 0.5)$$

$$a\_Var_{Species} \sim Normal(0, \sigma_{Species})$$

$$\sigma_{Species} \sim Cauchy(0, 1)$$

$$\sigma \sim Cauchy(0, 0.1)$$

Within species, I investigated the relationship between M values and log body mass and temperature using the following HMC simulations of 10,000 iterations, with 1000 warmup, 4 chains, and a thinning parameter of 1.

Model 2 - Temperature (variable n)

$$M_{est,i} \sim Normal(\mu_i, \sigma)$$

$$\mu_i = a + b_T \times T_{est,i}$$

$$M_{obs,i} \sim Normal(M_{est,i}, M_{sd,i})$$

$$T_{obs,i} \sim Normal(T_{est,i}, T_{sd,i})$$

$$a \sim Normal(0.25, 1)$$

$$b_T \sim Normal(0, 1)$$

$$\sigma \sim Cauchy(0, 1)$$

Model 3 - Body Mass (variable n)

$$M_{est,i} \sim Normal(\mu_i, \sigma)$$

$$\mu_i = a + b_W \times W$$

$$M_{obs,i} \sim Normal(M_{est,i}, M_{sd,i})$$

$$a \sim Normal(0.25, 1)$$

$$b_W \sim Normal(0, 1)$$

$$\sigma \sim Cauchy(0, 1)$$

I generated estimates of log mass-specific RMR using equation 1, inputting body mass, and temperature calculated for δ^{18}O. I modelled estimates of M values (M) as a linear function of estimates of log mass-specific RMR (RMR), using an HMC simulation of 10,000 iterations with 1000 warmup, 4 chains and a thinning parameter of 1.

Model 4 - Resting Metabolic Rate (n = 100)

$$M_{est,i} \sim Normal(\mu_i, \sigma)$$

$$\mu_i = a + b \times RMR_{est,i}$$

$$M_{obs,i} \sim Normal(M_{est,i}, M_{sd,i})$$

$$RMR_{obs,i} \sim Normal(RMR_{est,i}, RMR_{sd,i})$$

$$a \sim Normal(0.2, 1)$$

$$b \sim Normal(0, 10)$$

$$\sigma \sim Cauchy(0.1, 1)$$

4 Results

4.1 Relative Field Metabolic Rate Between Species

There was substantial overlap in M values between the six species of myctophids (figure 1). *K. anderssoni* ($M = 0.2468 \pm 0.0244$) *E. antarctica* ($M = 0.2312 \pm 0.0228$) and *G. braueri* ($M = 0.2201 \pm 0.0235$) had the highest estimates of species means of M , followed by *E. carlsbergi* ($M = 0.1959 \pm 0.0237$) and *P. bolini* ($M = 0.1888 \pm 0.0241$). *G. nicholsi* with had the lowest estimates for M ($M = 0.1548 \pm 0.0257$) (table 1).

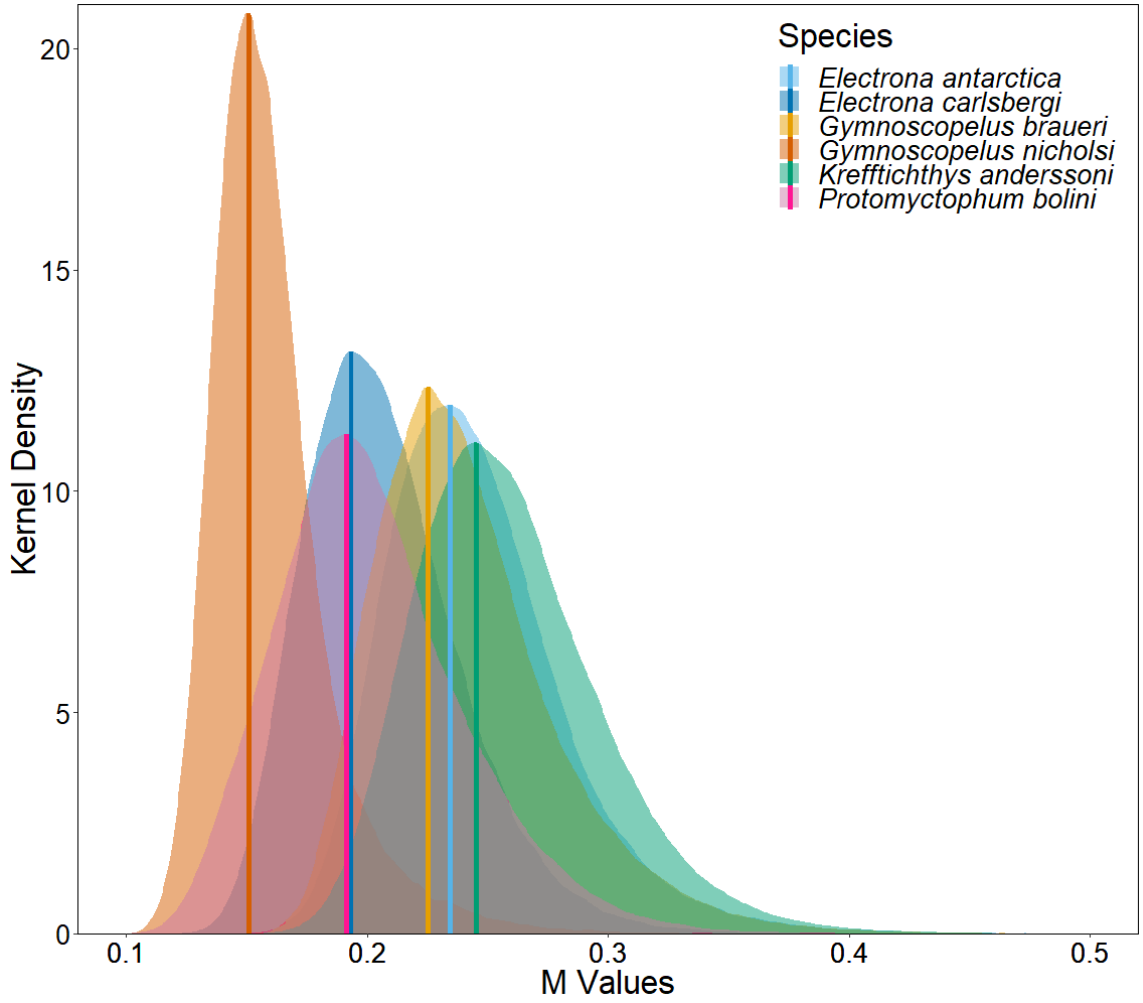

Figure 1: Kernel density of 10,000 estimates of M (a proxy for FMR) per individual fish, across 108 individuals, combined and grouped by six species. Maximum density of the distribution of each species is indicated by the solid lines.

Table 1: Posterior predictions of parameters for M values as a function of log body mass and reconstructed temperature (model 1), with convergence and mixing diagnostics: number of effective samples (N_eff) and $\hat{R}$. ELN = *Electrona antarctica*, ELC = *E. carlsbergi*, GYR = *Gymnoscopelus braueri*, GYN = *G. nicholsi*, KRA = *Krefftichthys anderssoni*, PRM = *Protomyctophum bolini*.

Parameter	Mean	SD	N_eff	$\hat{R}$
a_1	0.2066	0.0244	12997	1.00
b_W	0.0015	0.0137	15468	1.00
b_T	-0.002	0.0022	14438	1.00
a_Var_{ELN}	0.0246	0.0228	18448	1.00
a_Var_{ELC}	-0.0107	0.0237	11154	1.00
a_Var_{GYR}	0.0135	0.0235	6617	1.00
a_Var_{GYN}	-0.0518	0.0257	14264	1.00
a_Var_{KRA}	0.0402	0.0244	26605	1.00
a_Var_{PRM}	-0.0178	0.0241	7728	1.00
$\sigma_{Species}$	0.0480	0.0254	59093	1.00
σ	0.0036	0.0024	1529	1.00

Despite substantial overlap, the variable intercept of species was significantly greater than zero for *K. anderssoni*, and significantly less than zero for *G. nicholsi*, indicating that these species had higher and lower M values respectively, compared to other species (figure 2).

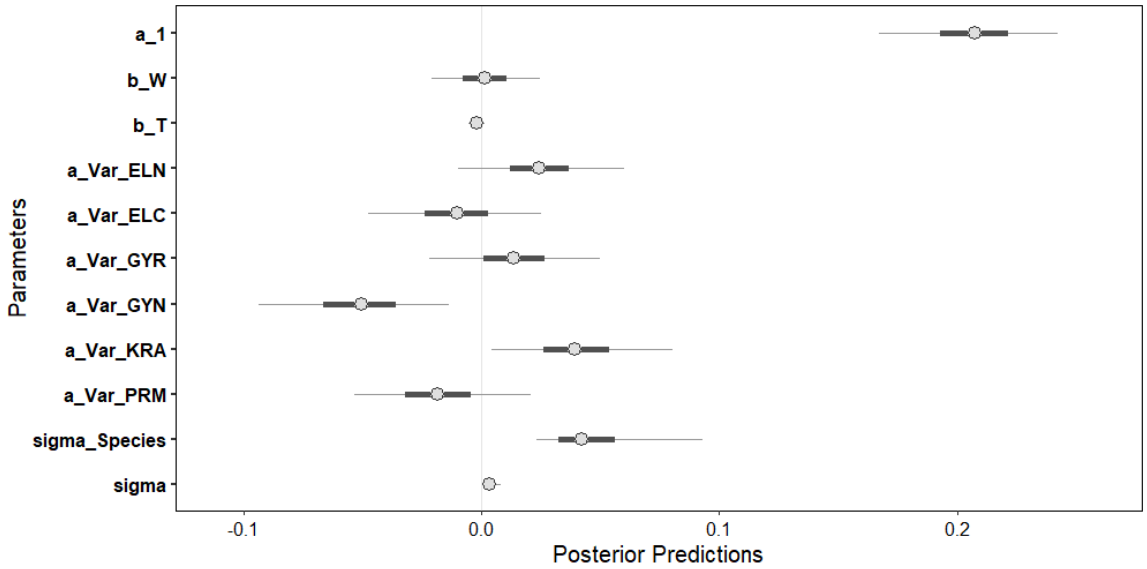

Figure 2: Posterior predictions for M values as a function of log body mass and reconstructed temperature (model 1), showing maximum density posterior interval (dot), 50% (thick line) and 90% (thin line) highest density posterior intervals. ELN = *Electrona antarctica*, ELC = *E. carlsbergi*, GYR = *Gymnoscopelus braueri*, GYN = *G. nicholsi*, KRA = *Krefftichthys anderssoni*, PRM = *Protomyctophum bolini*.

Supplementary analyses (appendix C) were unclear as to whether crushing whole otoliths, rather than milling, contributed to the lower δ^{13}C in *K. anderssoni*, and the resulting greater M values for this species.

4.2 M Values with Temperature and Body Mass

Posterior predictions of the scaling exponent of temperature for model 1 were negative (b_T = -0.0020 $\pm$0.0022). This suggests a slight negative linear relationship between M values and reconstructed temperature (figures 2 & 3, and table 1). There was no significant linear relationship between M values and log body mass (figures 2 & 3, and table 1).

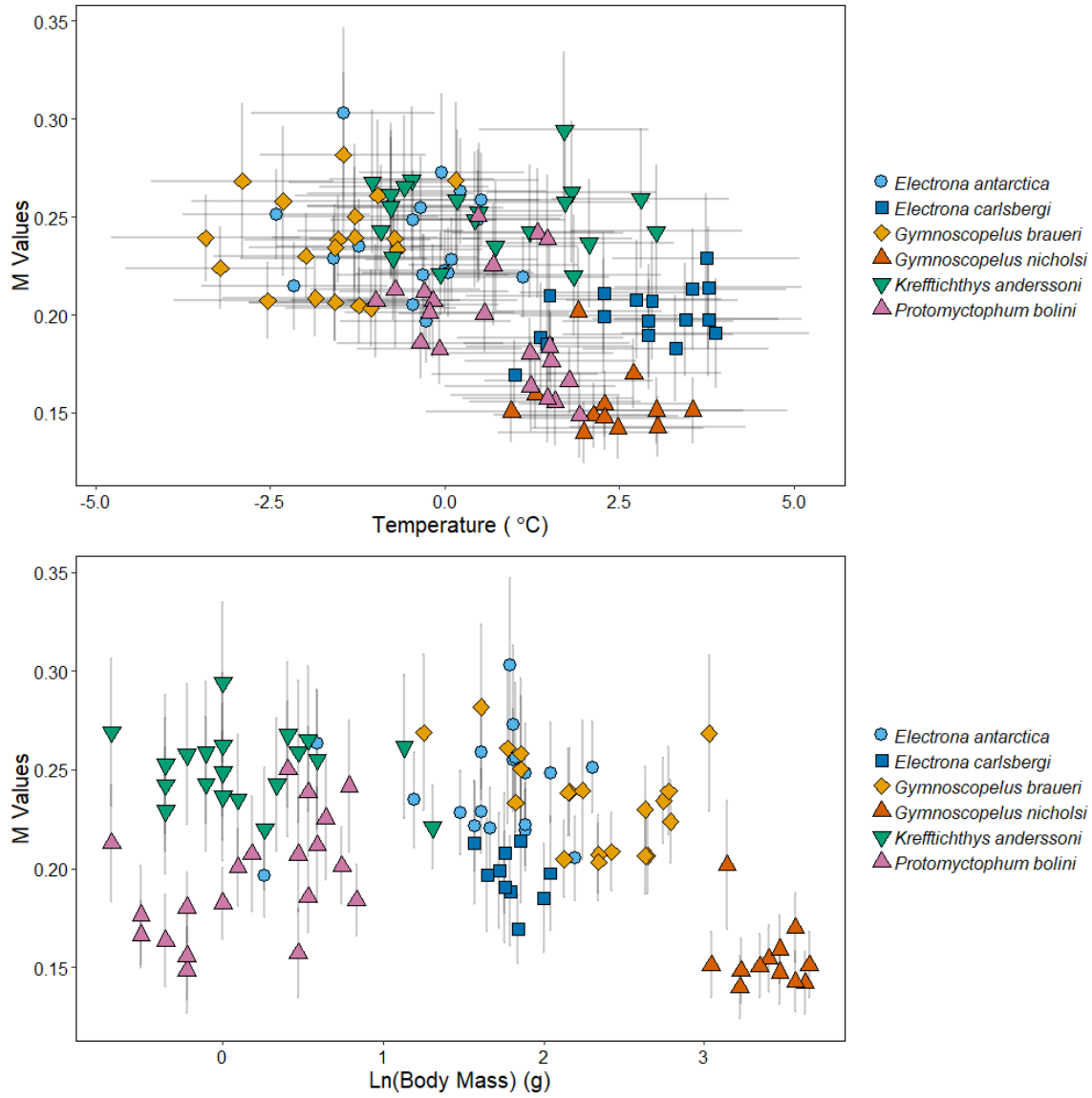

Figure 3: Maximum density of distributions of M values for individuals of six species of myctophids, with standard deviation bars, plotted against reconstructed temperature (°C) in the top graph and log body mass (g) in the bottom graph.

Within species, linear models of M values and temperature (model 2) converged for all species except for *E. carlsbergi* (table 2. In *P. bolini*, the scaling exponent was significantly greater than zero (b = -0.0089 ±0.0054), indicating that M values decreased with increasing temperature in this species (figures 4 and 5).

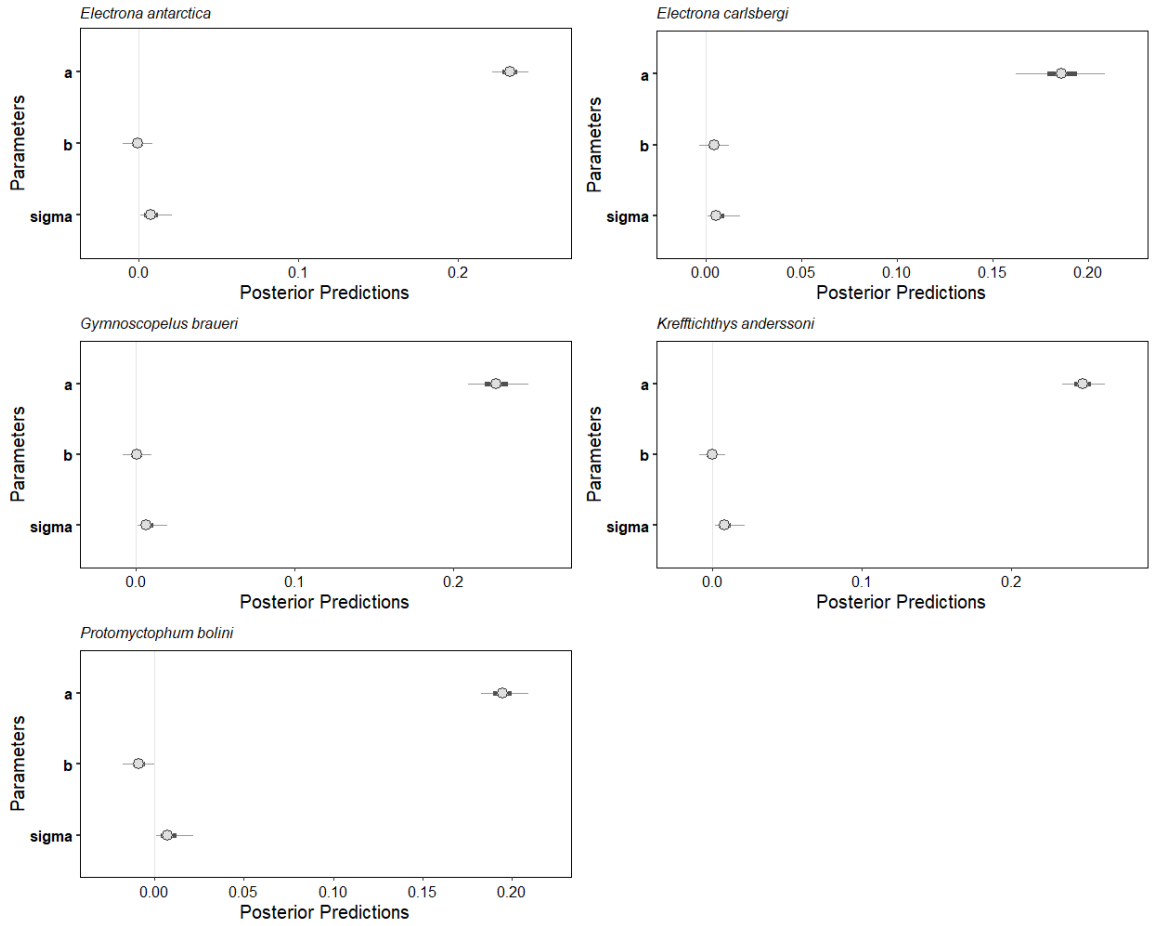

Figure 4: Posterior predictions for M values as a function of reconstructed temperature, within species (model 2), showing maximum density posterior interval (dot), 50% (thick line) and 90% (thin line) highest density posterior intervals.

Table 2: Posterior predictions of parameters from models of the relationship between temperature and M values within species (model 2), with convergence and mixing diagnostics: number of effective samples (N_eff) and $\hat{R}$. ELN = *Electrona antarctica*, ELC = *E. carlsbergi*, GYR = *Gymnoscopelus braueri*, GYN = *G. nicholsi*, KRA = *Krefftichthys anderssoni*, PRM = *Protomyctophum bolini*.

Species	**Parameter**	Mean	SD	N_eff	$\hat{R}$
ELN	a	0.2196	0.0208	4334	1.00
	b	0.0089	0.0122	4458	1.01
	σ	0.0099	0.0069	775	1.01
ELC	a	0.2695	0.1087	45	1.06
	b	-0.0442	0.0601	43	1.06
	σ	0.0065	0.0084	5	1.31
GYR	a	0.2275	0.0115	4489	1.00
	b	0.0007	0.0057	3553	1.00
	σ	0.0081	0.0060	852	1.00
GYN	a	0.1534	0.0133	6952	1.00
	b	-0.0007	0.0052	6654	1.00
	σ	0.0064	0.0049	1875	1.01
KRA	a	0.2481	0.0086	8133	1.00
	b	-0.0004	0.0054	5378	1.00
	σ	0.0091	0.0065	1015	1.01
PRM	a	0.1953	0.0080	3801	1.00
	b	-0.0089	0.0054	2922	1.00
	σ	0.0086	0.0066	889	1.00

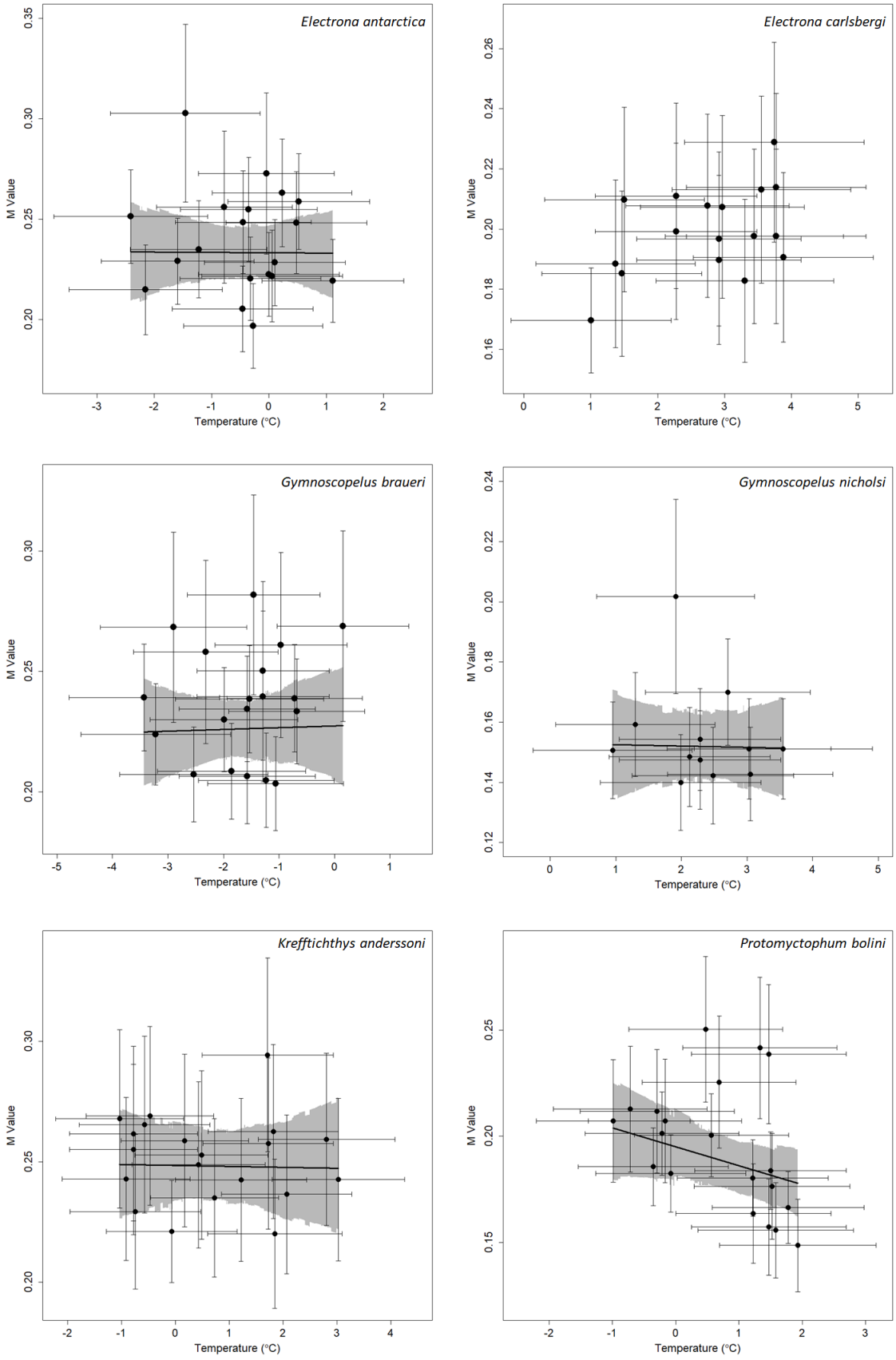

Figure 5: Resonstructed temperature and M values for each of the six species of myctophids. Where linear models converged (model 2), they are plotted with the means (solid line) and 95% highest density posterior interval (shaded areas).

Models of M values with log body mass converged for *E. antarctica, G. braueri* and *P. bolini* (table 3). Models for the other three species did not converge (section 6).

For *E. antarctica* and *G. braueri*, the scaling exponent was not significantly different from zero, suggesting that M was invariant with log body mass in these species. In *P. bolini*, the scaling exponent was significantly greater than zero (b = 0.0257 $\pm$0.0118), indicating a that M values increased with increasing log body mass (figures 6 and 7).

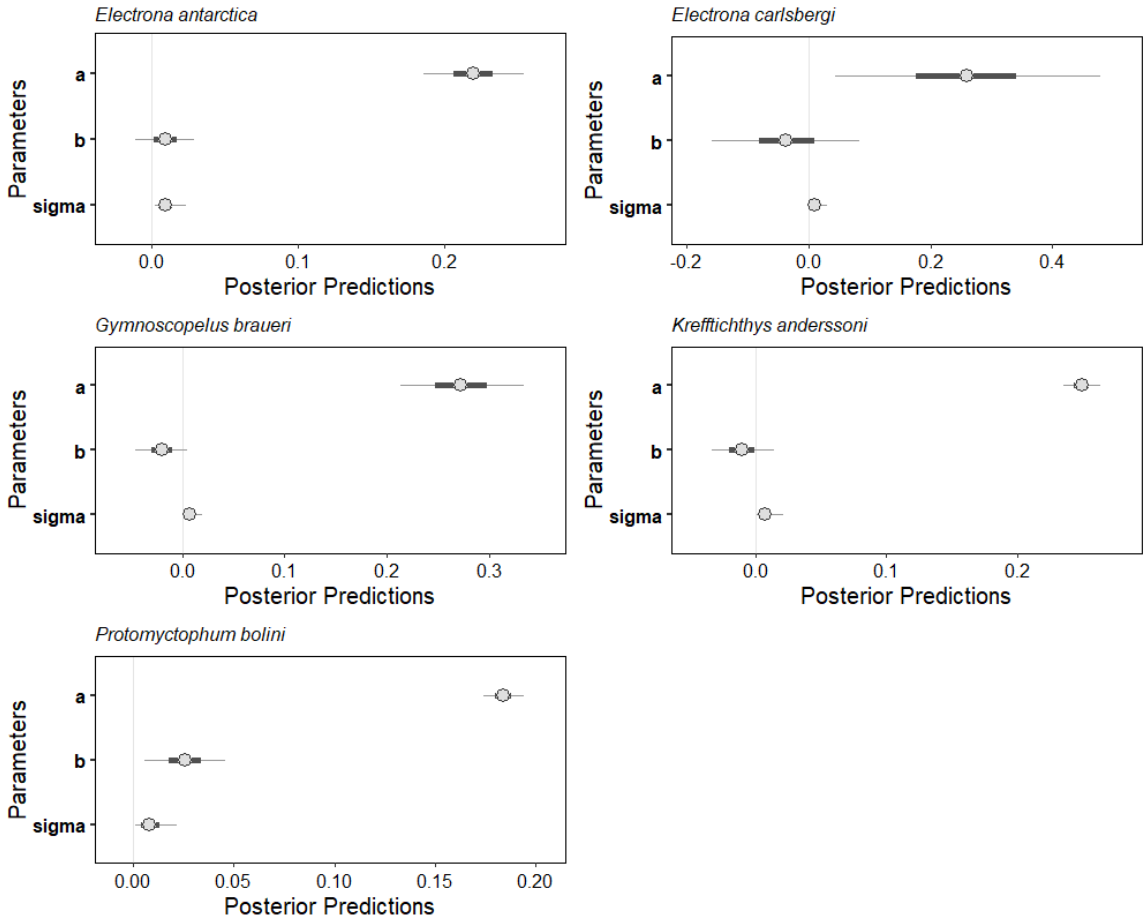

Figure 6: Posterior predictions for M values as a function of log body mass, within species (model 3), showing maximum density posterior interval (dot), 50% (thick line) and 90% (thin line) highest density posterior intervals.

Table 3: Posterior predictions of parameters from models of the relationship between log body mass and M values within species (model 3), with convergence and mixing diagnostics: number of effective samples (N_eff) and $\hat{R}$. ELN = *Electrona antarctica*, ELC = *E. carlsbergi*, GYR = *Gymnoscopelus braueri*, GYN = *G. nicholsi*, KRA = *Krefftichthys anderssoni*, PRM = *Protomyctophum bolini*.

Species	**Parameter**	Mean	SD	N_eff	$\hat{R}$
ELN	a	0.2196	0.0210	7053	1.00
	b	0.0090	0.0124	6692	1.00
	σ	0.0101	0.0069	1350	1.00
ELC	a	0.2586	0.1328	4735	1.00
	b	-0.0365	0.0734	45731	1.00
	σ	0.0121	0.0096	285	1.01
GYR	a	0.2720	0.0374	3454	1.00
	b	-0.0196	0.0156	3636	1.00
	σ	0.0086	0.0058	1203	1.01
GYN	a	0.1836	0.0996	131	1.03
	b	-0.0095	0.0292	127	1.03
	σ	0.0062	0.0052	60	1.05
KRA	a	0.2495	0.0087	2641	1.00
	b	-0.0101	0.0147	3538	1.00
	σ	0.0085	0.0065	765	1.01
PRM	a	0.1840	0.0061	5421	1.00
	b	0.0259	0.0122	6211	1.00
	σ	0.0094	0.0067	1174	1.00

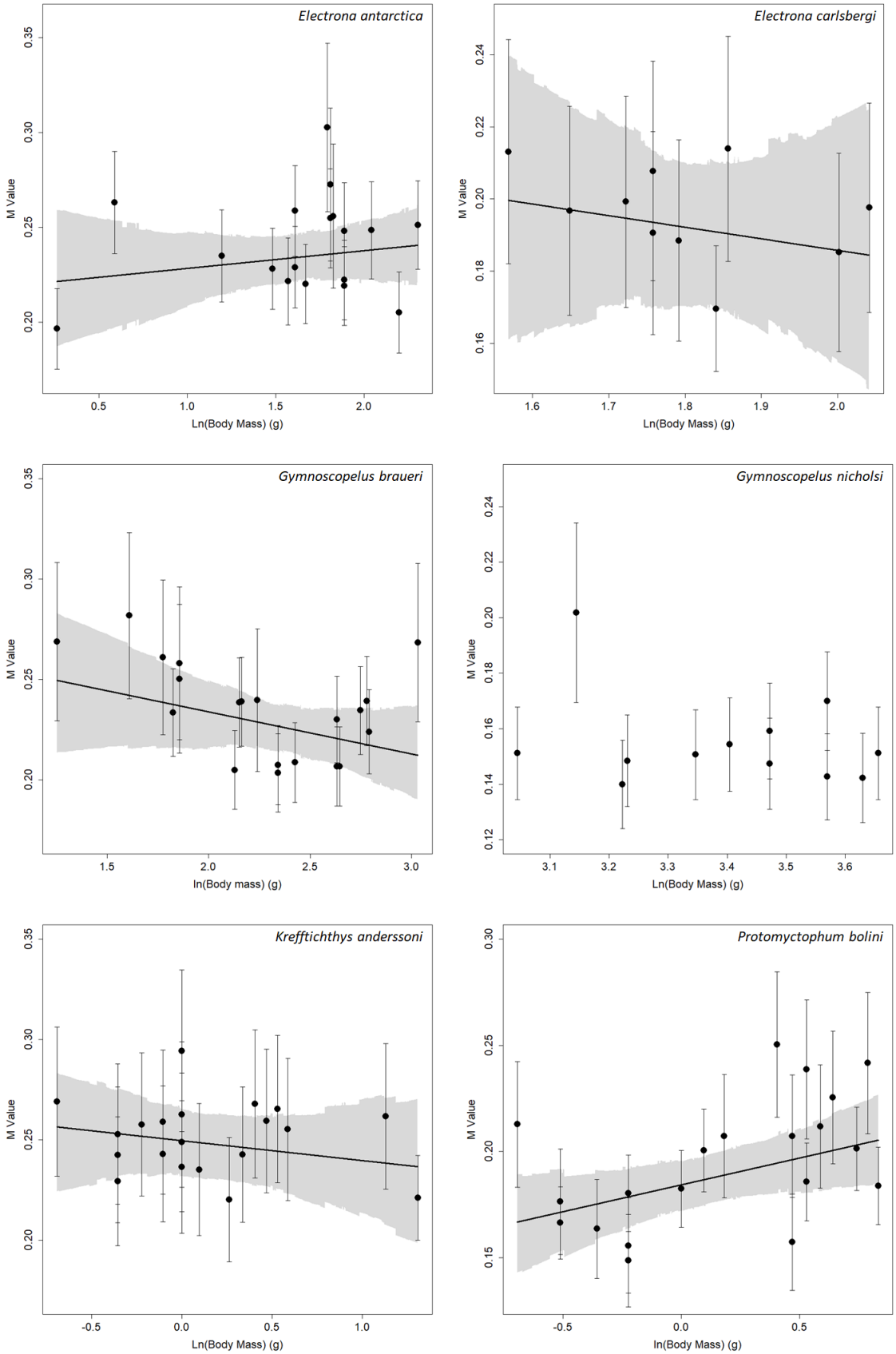

Figure 7: Log body mass (g) and M values for each of the six species. Where linear models (model 3) converged, they are plotted with the means (solid line) and 95% highest density posterior interval (shaded areas).

4.3 Comparsion of Estimates of Metabolic Rate

There was a significant negative correlation between estimates of log mass-specific RMR and M values (b = -0.0457 ±0.0071) (figure 8 and table 4), therefore M values decreased with increasing log mass-specific RMR (figure 9).

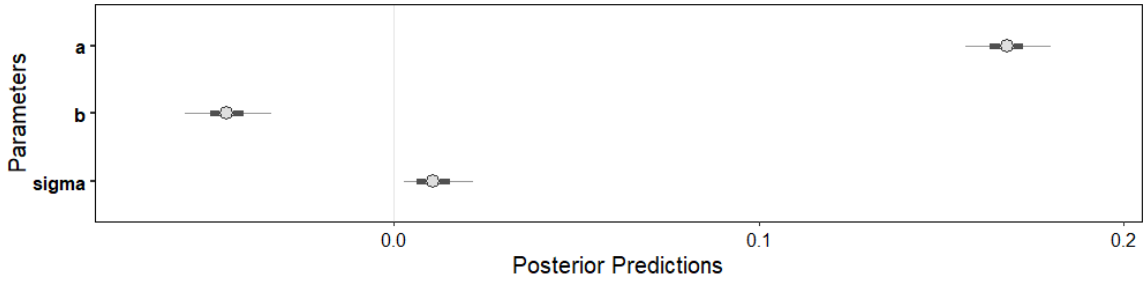

Figure 8: Posterior predictions for M values and log mass-specific RMR (model 4), showing maximum density posterior interval (dot), 50% (thick line) and 90% (thin line) highest density posterior intervals. ELN = *Electrona antarctica*, ELC = *E. carlsbergi*, GYR = *Gymnoscopelus braueri*, GYN = *G. nicholsi*, KRA = *Krefftichthys anderssoni*, PRM = *Protomyctophum bolini*.

Table 4: Posterior predictions of parameters for M values and log mass-specific RMR (model 4), with convergence and mixing diagnostics: number of effective samples (N_eff) and $\hat{R}$. ELN = *Electrona antarctica*, ELC = *E. carlsbergi*, GYR = *Gymnoscopelus braueri*, GYN = *G. nicholsi*, KRA = *Krefftichthys anderssoni*, PRM = *Protomyctophum bolini*.

Parameter	Mean	SD	N_eff	$\hat{R}$
a	0.1682	0.0072	901	1.01
b	-0.0457	0.0071	822	1.00
σ	0.0112	0.0059	244	1.01

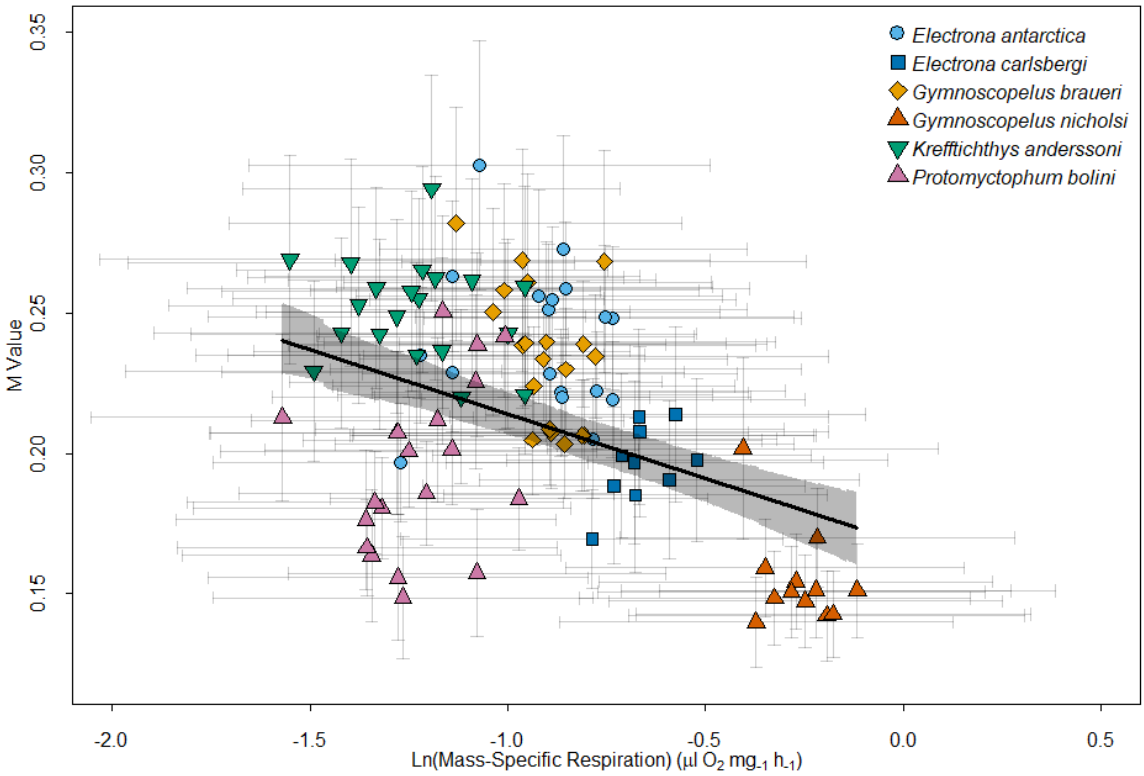

Figure 9: Relationship between estimates of log mass-specific standard metabolic rate, derived from equation 1 and M values, with standard deviation bars. Means (black line) and 95% highest density posterior intervals (shaded) of posterior predictions from model 4 are overlayed.

5 Discussion

5.1 Species Differences in Relative Field Metabolic Rate

This study showed that, despite overlap among them, species was the most useful variable in modelling M values. As temperature and body mass were accounted for, I theorise that this is due to differences in ecology among species. Field metabolic rate (FMR) comprises of basal metabolic costs and energy for growth, reproduction, digestion, excretion and movement (Treberg et al., 2016). While it is difficult to examine the other components of FMR, movement can be examined by comparing diel vertical migration strategies between species.

Different species of myctophids undertake diel vertical migration to different extents (Catul et al., 2011; Watanabe et al., 1999). *K. anderssoni, E. antarctica* and *G. braueri* are all known to perform diel vertical migration year round (Collins et al., 2008; Lourenço et al., 2017; Piatkowski et al., 1994; Saunders et al., 2015a; Torres and Somero, 1988b). These species also have a broad depth distribution, with individuals regularly found between 0-1000m depth (Gon and Heemstra, 1990; Pusch et al., 2004; Saunders et al., 2014). Individuals of these species are undertaking daily or near daily migrations across a large depth range, increasing the amount of respiration attributable to movement. This may account for the larger mean M values seen in these species.

In contrast, there is sparse evidence for diel vertical migration in *G. nicholsi* or *P. bolini* (Collins et al., 2008; Saunders et al., 2015b), and *E. carlsbergi* undertakes diel vertical migration only in the summer (Kozlov et al., 1991). Additionally, while individuals of these species are still occasionally found down to 1000m depth, the majority of the population stays above 700m in the case of *G. nicholsi* (Gon and Heemstra, 1990; Pusch et al., 2004; Saunders et al., 2015a), or above 400m for *P. bolini* and *E. carlsbergi* (Collins et al., 2012; Kozlov et al., 1991; Pusch et al., 2004; Saunders et al., 2014, 2015b). Given that these species are less likely to complete daily/near

daily migrations, and if they do, are likely to be migrating across more compressed depth ranges, they are likely to have less respiration attributable to movement, which may explain their lower mean M values. Furthermore, there is evidence that *G. nicholsi* individuals may become benthopelagic (living near the seafloor) during late adulthood (Gon and Heemstra, 1990; Saunders et al., 2015a). This would reduce their movement compared to pelagic (living in the water column away from the seafloor) fishes, resulting in a lower FMR, and could explain why this species had significantly lower$M$ values than the other five species.

5.2 Temperature and Body Mass

There was a slight negative relationship between temperature and M values, which may be an artefact of differing ecological factors between species. Species with the lowest mean M values (*G. nicholsi*, *P. bolini* and *E. carlsbergi*) are more common in the north of the Scotia Sea, where water temperatures are warmer. (Collins et al., 2012; Gon and Heemstra, 1990; Piatkowski et al., 1994; Saunders et al., 2014, 2015b). There is also evidence that these species do not complete their life cycles within the Scotia Sea, as the temperatures are too low for the more sensitive larval stages. Recruitment for these species may occur outside of the Scotia Sea, with adults migrating in from elsewhere (Collins et al., 2008, 2012; Saunders et al., 2014, 2015a). This would mean that these species are living at the lowest end of their thermal range, which may inhibit their metabolic rates (Clarke and Johnston, 1999; Killen et al., 2010; Pörtner and Farrell, 2008).

In contrast, species with the highest mean M values (*K. anderssoni, E. antarctica* and *G. braueri*) are more common in the colder, more southerly waters of the Scotia Sea. These species are truly Antarctic, with all life stages found in the Scotia Sea (Collins et al., 2008, 2012; Gon and Heemstra, 1990; Lourenço et al., 2017; Saunders et al., 2014, 2015a). Individuals of these species are more likely to be living well within their thermal range, and therefore able to maintain higher metabolic rates, explaining the higher M values (Clarke and Johnston, 1999; Killen et al., 2010;

Pörtner and Farrell, 2008). More research on otoliths from individuals of *G. nicholsi*, *P. bolini* and *E. carlsbergi* from sites north of the Scotia Sea would be needed to to confirm this theory. However, given that temperature was not significantly correlated with M values within most species, and that species captured the most variation in M values, it seems likely that any negative correlation between species is an artefact.

Within species, log body mass and temperature were only significantly correlated with M values in *P. bolini*. Within *P. bolini*, M values increased with increasing log body mass, and decreased with increasing temperature. This is the opposite of what would be expected according to metabolic theory, and relationships of M values with log body mass and temperature in previous studies, where mass-specific metabolic rate, and therefore M values, decreased with increasing body mass, and increased with increasing temperature (Brown et al., 2004; Clarke and Johnston, 1999; Killen et al., 2010; Pörtner and Farrell, 2008; Trueman et al., 2016). The reason for this is unclear, and more measurements of M values in this species, across a range of body masses, would be needed to investigate this further.

5.3 Resting and Field Metabolic Rate

The negative linear relationship of M values and log mass-specific resting metabolic rate (RMR) suggests that fishes with a high RMR have a low FMR, contrary to previous studies and metabolic theories (Brown et al., 2004; Killen et al., 2016). If we assume that equation 1 generates reasonable estimates for values of log mass-specific RMR, this suggests that the other components of FMR (thermic effect of food, growth, reproduction, movement and excretion) have a larger influence on FMR than RMR does. These factors are more likely to be influenced by ecological differences among species, and this is supported by the result that species had the greatest influence on M values.

There are issues with how the equation was parameterised which may affect any inferences drawn from it. Two of the studies used to parameterise equation 1

gave mass-specific RMR based on electron transport system activity (ETS) (Belcher et al., 2019). ETS is converted to mass-specific RMR using ratios which varied between the two studies. For example, one study used an ETS/RMR ratio of 2,(Ariza et al., 2015) while another used a ratio of 1.16 (Ikeda, 1989). The ETS/RMR ratio of 2 was used based on a study of zooplankton, (Hernández-Leó and Gómez, 1996) while the ETS/RMR ratio of 1.16 was based the author's results from gobies (family Gobiidae) and pomacentrids (family Pomacentridae). Uncertainty around the ETS/RMR ratio was not accounted for when calculating log mass-specific RMR from ETS, and consequently was not incorporated when parameterising equation 1. Studies used to parameterise equation 1 had a much greater temperature range (0.5 to 20 °C) than was estimated for the fishes in our study (-3.4 to 3.9 °C, maximum density posterior values). This may have overinflated the postive relationship between metabolic rate and temperature when comparing fishes from the relatively narrow range of temperatures in the Scotia Sea.

Variation in M values, and therefore FMR, is not adequately captured using log body mass, temperature or estimated log RMR as predictors. Given this, and the discussed issues in parameterisation, equation 1 is not adequate enough in accurately predicting metabolic rate to be used in carbon modelling. Ecological factors such as migratory strategy are likely to be better predictors of FMR, but more research is needed across a wider range of species to confirm which ecological factors have the most influence on FMR.

6 Future Work

This work will become one of the chapters of my thesis, and the first paper from my PhD project. When rewriting, I will make two main changes.

First, sensitivity analysis for M values across a range of species (appendix E) indicated that $\delta^{13}C_{phytoplankton}$, which is used to estiamte $\delta^{13}C_{diet}$ had the greatest influence on the maximum density of M. The δ^{13}C value of muscle tissue, corrected for trophic fractionation factor, is a reasonable approximation of the $\delta^{13}C_{diet}$ of an individual fish (DeNiro and Epstein, 1978). Each otolith used in this study also came with muscle tissue, which has been analysed for δ^{13}C. Unfortunately, these data were not available when this report was in preparation. However, for the thesis chapter and paper manuscript, M values will be recalculated using this data, ensuring a more accurate and precise estimate for each fish. I will also work on putting the M and temperature functions into a Bayesian framework.

Many Hamiltonian Monte Carlo (HMC) simulations in this study did not converge. In future analyses, for my thesis chapter and when this is written into a paper, I will run HMC with a single, long chain, as opposed to four short chains, as was done with model 1. I will also re-examine the priors and thinning parameters used in this model.

7 Thesis Plan and Gantt Chart

7.1 Overview of PhD

The broad aim of my PhD is to investigate how the field metabolic rate (FMR) of fishes varies at a macroecological scale. The work in this report forms the basis for chapter four of my PhD thesis and a research paper. Target journals for this paper are Marine Ecology Progress Series, Journal of Fish Biology or Polar Biology.

Aside from this and an introduction (chapter one), I plan on three other chapters, outlined here. Each chapter, apart from the introduction, will be written up into a paper.

7.2 Chapter 2: M Values Dataset

The first step of my PhD has been to build up a dataset of M values from otolith isotope δ^{13}C from a range of species of fishes across a range of ecological categories and taxonomy. The dataset currently consists of 42 species, with otoliths from a further 25 species awaiting stable isotope analysis. Each species is represented by otoliths from ten individuals, and must have associated catch location and year, and a measure of body size. The majority of the stable isotope analysis will take place in late 2019, when I visit the Life Sciences Mass Spectrometry Facility (figure 10). The dataset presently has good representation across benthopelagic (fishes living near seafloor) and deep-sea fishes, but is lacking in pelagic (fishes living in the water column away from the seafloor) and migratory fishes. I am working on filling this gap by forming collaborations with other otolith researchers, and collecting otoliths from the Split fish market in Croatia. Once other papers are published, we will publish this dataset as a data paper, to make it available to the wider scientific community. Target journals for this paper are Ecology, PLOS One or Ecological Research.

7.3 Chapter 3: Body Mass and Temperature Scaling

There are several theories as to how metabolic rate scales with body mass and temperature, and how it varies between species, including the metabolic theory of ecology (Brown et al., 2004) and the metabolic level boundaries hypothesis (Glazier, 2005). These theories are used to predict how species might respond to climate change, and were initially developed using basal metabolic rate (BMR) data from endotherms, analogous to standard or resting metabolic rate (RMR) in ectotherms. As discussed in the above report, FMR is the more appropriate measure of metabolic rate in a modelling context.

There have been no studies examining how body mass and temperature scale with FMR in fishes. The common method for studying FMR in endotherms, the doubly-labelled water technique does not work in fishes, due to their high water turnover rates (Treberg et al., 2016). The otolith isotope technique for M values, is ideal for investigating FMR at a macroecological scale, as otoliths archives are numerous, primarly due to their use in ageing fishes (Campana, 1999). I will use phylogenetic comparative methods to account for phylogenetic non-independence; the principle that species are not independent data points, due to their shared evolutionary history (Harvey and Pagel, 1991). Target journals for this paper are Ecology Letters, Biology Letters or Journal of Animal Ecology.

7.4 Chapter 5: Ecological Influences on M Values

From reading previous macroecological studies of fish metabolic rate, I am interested in which ecological factors significantly influence M values, and therefore FMR. Ecological factors I will examine are habitat (benthic, benthopelagic or pelagic), (Killen et al., 2010, 2016) depth, (Drazen and Seibel, 2007; Killen et al., 2010, 2016; Seibel and Drazen, 2007) body shape, (Sherwood and Rose, 2003; Uyeda et al., 2017) migratory habits and schooling or shoaling behaviours. I will also investigate whether M values correlated with growth, as estimated through the k term in the von Bertalanffy

growth equation. As with chapter three, I will use phylogenetic comparitive methods in my analysis. I will also compare M values across the fish phylogenetic tree. This chapter and paper may split into several, depending on the results of the analyses. Target journals for this paper are Proceedings of the Royal Society B, Ecology and Evolution or Marine Ecology Progress Series.

7.5 Gantt Chart

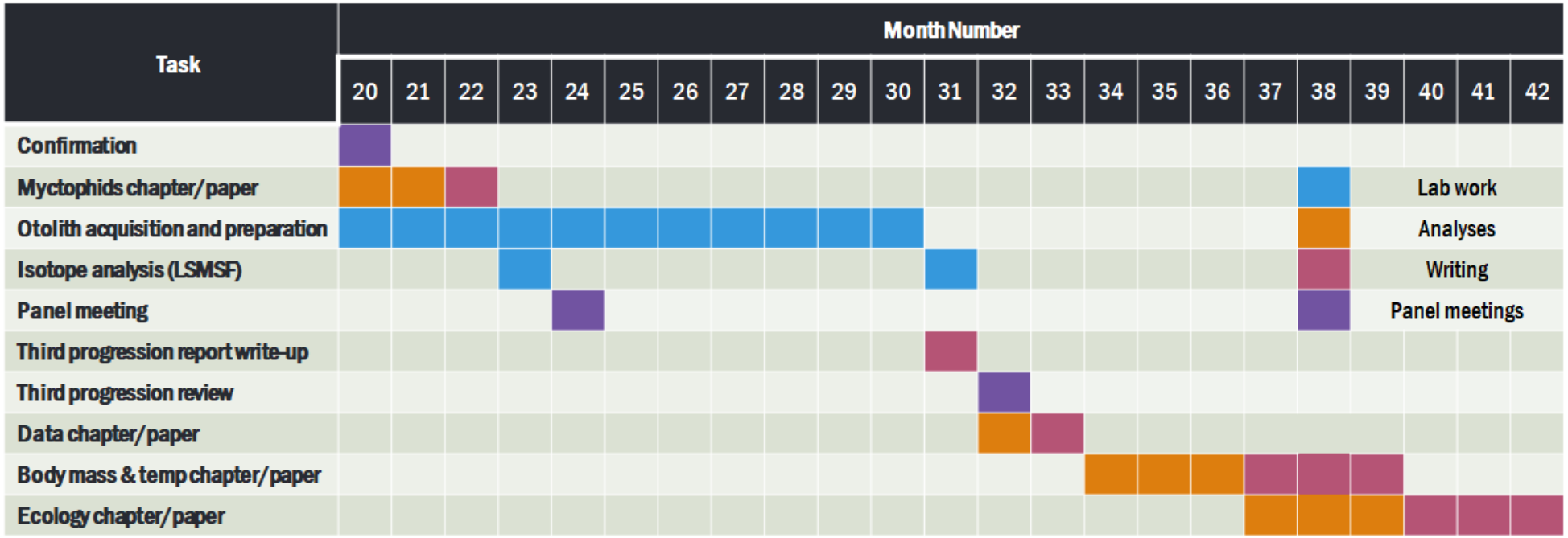

Figure 10: Gantt chart of expected progress until the end of my PhD.

8 Acknowledgements

Thank you to Dr. Gabriele Stowasser and the British Antarctic Survey for donating the otoliths used in this study. Special thanks to my supervisors Dr. Clive Trueman, Dr. Natalie Cooper and Mr. Oliver Crimmen for their ongoing support with all my research, and for providing constructive feedback on earlier versons of this report. Assistance in mounting the otoliths provided by Mr. Joseph Jones, Mr. Daniel Doran and Mr. Matthew Beverley-Smith is greatly appreciated. Thank you also to Mr. Bastian Hambach and Mrs. Megan Wilding for running the stable isotope analyses. This work is supported by the Natural Enviornment Research Council [grant number NE/L002531/1].

References

T. R. Anderson, A. P. Martin, R. S. Lampitt, C. N. Trueman, S. A. Henson, and D. J. Mayor. Quantifying carbon fluxes from primary production to mesopelagic fish using a simple food web model. *ICES Journal of Marine Science*, 2018.

A. Ariza, J. C. Garijo, J. M. Landeira, F. Bordes, and S. Hernndez-Len. Migrant biomass and respiratory carbon flux by zooplankton and micronekton in the subtropical northeast Atlantic Ocean (Canary Islands). *Progress in Oceanography*, 134:330–342, 2015. ISSN 0079-6611. doi: https://doi.org/10.1016/j.pocean.2015.03.003. URL `http://www.sciencedirect.com/science/article/pii/S0079661115000440`.

A. Belcher, R. A. Saunders, and G. A. Tarling. Respiration rates and active carbon flux of mesopelagic fishes (Family Myctophidae) in the Scotia Sea, Southern Ocean. *Marine Ecology Progress Series*, 610:149–162, 2019. ISSN 0171-8630. doi: 10.3354/meps12861. URL `<Go to ISI>://WOS:000464515700011`.

J. H. Brown, J. F. Gillooly, A. P. Allen, V. M. Savage, and G. B. West. Toward a metabolic theory of ecology. *Ecology*, 85(7):1771–1789, 2004.

L. M. Cammen, S. Corwin, and J. P. Christensen. Electron transport system (ETS) activity as a measure of benthic macrofaunal metabolism. *Mar. Ecol. Prog. Ser*, 65 (1):171–182, 1990.

S. E. Campana. Chemistry and composition of fish otoliths: pathways, mechanisms and applications. *Marine Ecology Progress Series*, 188:263–297, 1999. ISSN 01718630, 16161599. URL `http://www.jstor.org/stable/24853344`.

V. Catul, M. Gauns, and P. K. Karuppasamy. A review on mesopelagic fishes belonging to family Myctophidae. *Reviews in Fish Biology and Fisheries*, 21(3): 339–354, 2011. ISSN 0960-3166. doi: 10.1007/s11160-010-9176-4. URL `<Go to ISI>://WOS:000293398600003`.

M. T. Chung, C. N. Trueman, J. A. Godiksen, and P. Grønkjær. Otolith delta13C values as a metabolic proxy: approaches and mechanical underpinnings. *Marine*

and Freshwater Research, pages –, 2019a. doi: https://doi.org/10.1071/MF18317. URL https://www.publish.csiro.au/paper/MF18317.

M. T. Chung, C. N. Trueman, J. A. Godiksen, M. E. Holmstrup, and P. Grønkjær. Field metabolic rates of teleost fishes are recorded in otolith carbonate. *Communications biology*, 2(1):24, 2019b. ISSN 2399-3642.

A. Clarke and N. M. Johnston. Scaling of metabolic rate with body mass and temperature in teleost fish. *Journal of Animal Ecology*, 68(5):893–905, 1999. ISSN 1365-2656. doi: 10.1046/j.1365-2656.1999.00337.x. URL http://dx.doi.org/10.1046/j.1365-2656.1999.00337.x.

M. A. Collins, J. C. Xavier, N. M. Johnston, A. W. North, P. Enderlein, G. A. Tarling, C. M. Waluda, E. J. Hawker, and N. J. Cunningham. Patterns in the distribution of myctophid fish in the northern Scotia Sea ecosystem. *Polar Biology*, 31(7):837–851, 2008. ISSN 0722-4060.

M. A. Collins, G. Stowasser, S. Fielding, R. Shreeve, J. C. Xavier, H. J. Venables, P. Enderlein, Y. Cherel, and A. Van de Putte. Latitudinal and bathymetric patterns in the distribution and abundance of mesopelagic fish in the Scotia Sea. *Deep Sea Research Part II: Topical Studies in Oceanography*, 59-60:189–198, 2012. ISSN 0967-0645. doi: https://doi.org/10.1016/j.dsr2.2011.07.003. URL http://www.sciencedirect.com/science/article/pii/S0967064511001858.

P.C. Davison, D.M. Checkley Jr, J.A. Koslow, and J. Barlow. Carbon export mediated by mesopelagic fishes in the northeast Pacific Ocean. *Progress in Oceanography*, 116:14–30, 2013. ISSN 0079-6611.

M. J. DeNiro and S. Epstein. Influence of diet on the distribution of carbon isotopes in animals. *Geochimica et Cosmochimica Acta*, 42(5):495–506, 1978. ISSN 0016-7037. doi: https://doi.org/10.1016/0016-7037(78)90199-0. URL http://www.sciencedirect.com/science/article/pii/0016703778901990.

J. Donnelly and J.J. Torres. Oxygen consumption of midwater fishes and crustaceans

from the eastern Gulf of Mexico. *Marine Biology*, 97(4):483–494, 1988. ISSN 0025-3162.

J. C. Drazen and B. A. Seibel. Depthrelated trends in metabolism of benthic and benthopelagic deepsea fishes. *Limnology and Oceanography*, 52(5):2306–2316, 2007. ISSN 1939-5590.

R. Froese and D. Pauly. Fishbase, 2019. URL `https://www.fishbase.in/`.

D. S. Glazier. Beyond the 3/4-power law: variation in the intra-and interspecific scaling of metabolic rate in animals. *Biological Reviews*, 80(4):611–662, 2005. ISSN 1469-185X.

O. Gon and P. C. Heemstra. *Fishes of the Southern Ocean*, volume 1. JLB Smith Institute of Ichthyology Grahamstown, 1990.

P. Harvey and M. D. Pagel. *The comparative method in evolutionary biology*, volume 239. Oxford university press Oxford, 1991.

Santiago Hernández-Leó and May Gómez. Factors affecting the respiration/ETS ratio in marine zooplankton. *Journal of Plankton Research*, 18(2):239–255, 1996.

H. Høie, E. Otterlei, and A. Folkvord. Temperature-dependent fractionation of stable oxygen isotopes in otoliths of juvenile cod (*Gadus morhua* l.). *ICES Journal of Marine Science*, 61(2):243–251, 2004. ISSN 1095-9289.

T. Ikeda. Estimated respiration rate of myctophid fish from the enzyme activity of the electron-transport-system. *Journal of the Oceanographical Society of Japan*, 45 (3):167–173, 1989. ISSN 0029-8131.

S. S. Killen, D. Atkinson, and D. S. Glazier. The intraspecific scaling of metabolic rate with body mass in fishes depends on lifestyle and temperature. *Ecology Letters*, 13(2):184–193, 2010. doi: doi:10.1111/j.1461-0248.2009.01415.x. URL `https://onlinelibrary.wiley.com/doi/abs/10.1111/j.1461-0248.2009.01415.x`.

S. S. Killen, D. S. Glazier, E. L. Rezende, T. D. Clark, D. Atkinson, A. S. T. Willener, and L. G. Halsey. Ecological influences and morphological cor-

relates of resting and maximal metabolic rates across teleost fish species. *The American Naturalist*, 187(5):592–606, 2016. doi: 10.1086/685893. URL https://www.journals.uchicago.edu/doi/abs/10.1086/685893.

A.N. Kozlov, K.V. Shust, and A.V. Zemsky. Seasonal and inter-annual variability in the distribution of *Electrona carlsbergi* in the Southern Polar Front area (the area to the north of south georgia is used as an example). *CCAMLR Science*, 7:337–368, 1991.

S. Lourenço, R. A. Saunders, M. Collins, R. Shreeve, C. A. Assis, M. Belchier, J. L. Watkins, and J. C. Xavier. Life cycle, distribution and trophodynamics of the lanternfish *Krefftichthys anderssoni* (lönnberg, 1905) in the Scotia Sea. *Polar Biology*, 40(6):1229–1245, 2017. ISSN 0722-4060.

S. Magozzi, A. Yool, H.B. Vander Zanden, M.B. Wunder, and C.N. Trueman. Using ocean models to predict spatial and temporal variation in marine carbon isotopes. *Ecosphere*, 8(5):e01763, 2017. ISSN 2150-8925.

R. McElreath. rethinking: Statistical Rethinking book package, 2016. R package version 1.59.

O. Mersmann, H. Trautmann, D. Steuer, and B. Bornkamp. *truncnorm: Truncated Normal Distribution*, 2018. URL https://CRAN.R-project.org/package=truncnorm. R package version 1.0-8.

U. Passow and C. A. Carlson. The biological pump in a high CO2 world. *Marine Ecology Progress Series*, 470:249–271, 2012.

U. Piatkowski, P. G. Rodhouse, M. G. White, D. G. Bone, and C. Symon. Nekton community of the Scotia Sea as sampled by the RMT 25 during austral summer. *Marine Ecology Progress Series*, 112:13–28, 1994. ISSN 0171-8630.

H. O. Pörtner and A. P. Farrell. Physiology and climate change. *Science*, pages 690–692, 2008. ISSN 0036-8075.

C. Pusch, P. A. Hulley, and K. H. Kock. Community structure and feeding ecology of mesopelagic fishes in the slope waters of King George Island (South Shetland Islands, Antarctica). *Deep Sea Research Part I: Oceanographic Research Papers*, 51(11):1685–1708, 2004. ISSN 0967-0637. doi: https://doi.org/10.1016/j.dsr.2004.06.008. URL http://www.sciencedirect.com/science/article/pii/S0967063704001177.

R Core Team. R: A language and environment for statistical computing, 2018. URL https://www.R-project.org/. version 3.4.4.

R. A. Saunders, M. A. Collins, E. Foster, R. Shreeve, G. Stowasser, P. Ward, and G. A. Tarling. The trophodynamics of Southern Ocean Electrona (Myctophidae) in the Scotia Sea. *Polar biology*, 37(6):789–807, 2014. ISSN 0722-4060.

R. A. Saunders, M. A. Collins, P. Ward, G. Stowasser, R. Shreeve, and G. A. Tarling. Distribution, population structure and trophodynamics of Southern Ocean Gymnoscopelus (Myctophidae) in the Scotia Sea. *Polar Biology*, 38(3):287–308, 2015a. ISSN 0722-4060.

R. A. Saunders, M. A. Collins, P. Ward, G. Stowasser, R. Shreeve, and G. A. Tarling. Trophodynamics of Protomyctophum (Myctophidae) in the Scotia Sea (Southern Ocean). *Journal of Fish Biology*, 87(4): 1031–1058, 2015b. ISSN 0022-1112. doi: 10.1111/jfb.12776. URL https://onlinelibrary.wiley.com/doi/abs/10.1111/jfb.12776.

G. A. Schmidt, G. R. Bigg, and E. J. Rohling. Global seawater oxygen-18 database, 1999. URL https://data.giss.nasa.gov/o18data/. version 1.22.

B. A. Seibel and J. C. Drazen. The rate of metabolism in marine animals: environmental constraints, ecological demands and energetic opportunities. *Philosophical Transactions of the Royal Society B: Biological Sciences*, 362(1487):2061–2078, 2007. ISSN 0962-8436.

G. D. Sherwood and G. A. Rose. Influence of swimming form on otolith delta13C in marine fish. *Marine Ecology Progress Series*, 258:283–289, 2003. ISSN 0171-8630.

C. T. Solomon, P. K. Weber, J. J. Cech, Jr., B. L. Ingram, M. E. Conrad, M. V. Machavaram, A. R. Pogodina, and R. L. Franklin. Experimental determination of the sources of otolith carbon and associated isotopic fractionation. *Canadian Journal of Fisheries and Aquatic Sciences*, 63(1):79–89, 2006. ISSN 0706-652X. doi: 10.1139/f05-200. URL https://doi.org/10.1139/f05-200.

M. A. St. John, A. Borja, G. Chust, M. Heath, I. Grigorov, P. Mariani, A. P. Martin, and R. S. Santos. A dark hole in our understanding of marine ecosystems and their services: Perspectives from the mesopelagic community. *Frontiers in Marine Science*, 3(31), 2016. ISSN 2296-7745. doi: 10.3389/fmars.2016.00031. URL https://www.frontiersin.org/article/10.3389/fmars.2016.00031.

Stan Development Team. RStan: the R interface to Stan, 2018. URL http://mc-stan.org/. R package version 2.17.3.

A. Tagliabue and L. Bopp. Towards understanding global variability in ocean carbon13. *Global Biogeochemical Cycles*, 22(1), 2008. ISSN 1944-9224.

S. R. Thorrold, S. E. Campana, C. M. Jones, and P. K. Swart. Factors determining delta c-13 and delta o-18 fractionation in aragonitic otoliths of marine fish. *Geochimica Et Cosmochimica Acta*, 61(14):2909–2919, 1997. ISSN 0016-7037. doi: 10.1016/s0016-7037(97)00141-5. URL <Go to ISI>://WOS:A1997XT45500009.

J.J. Torres and G.N. Somero. Metabolism, enzymic activities and cold adaptation in Antarctic mesopelagic fishes. *Marine Biology*, 98(2):169–180, 1988a. ISSN 0025-3162.

J.J. Torres and G.N. Somero. Vertical distribution and metabolism in Antarctic mesopelagic fishes. *Comparative Biochemistry and Physiology–Part B: Biochemistry and Molecular Biology*, 90(3):521–528, 1988b. ISSN 0305-0491.

J.J Torres, B.W. Belman, and J.J. Childress. Oxygen consumption rates of midwater fishes as a function of depth of occureence. *Deep Sea Research Part A. Oceanographic Research Papers*, 26(2):185–197, 1979.

J. R. Treberg, S. S. Killen, T. J. MacCormack, S. G. Lamarre, and E. C. Enders. Estimates of metabolic rate and major constituents of metabolic demand in fishes under field conditions: Methods, proxies, and new perspectives. *Comparative Biochemistry and Physiology a-Molecular & Integrative Physiology*, 202: 10–22, 2016. ISSN 1095-6433. doi: 10.1016/j.cbpa.2016.04.022. URL <Go to ISI>://WOS:000389110800003.

C. N. Trueman, G. Johnston, B. O'Hea, and K. M. MacKenzie. Trophic interactions of fish communities at midwater depths enhance long-term carbon storage and benthic production on continental slopes. *Proceedings of the Royal Society B: Biological Sciences*, 281(1787):20140669, 2014. doi: doi:10.1098/rspb.2014.0669. URL https://royalsocietypublishing.org/doi/abs/10.1098/rspb.2014.0669.

C. N. Trueman, M. T. Chung, and D. Shores. Ecogeochemistry potential in deep time biodiversity illustrated using a modern deep-water case study. *Philosophical Transactions of the Royal Society B: Biological Sciences*, 371(1691), 2016. doi: 10.1098/rstb.2015.0223.

J. C. Uyeda, M. W. Pennell, E. T. Miller, R. Maia, and C. R. McClain. The evolution of energetic scaling across the vertebrate tree of life. *The American Naturalist*, 190(2):185–199, 2017. doi: 10.1086/692326. URL http://www.journals.uchicago.edu/doi/abs/10.1086/692326.

H. Watanabe, M. Moku, K. Kawaguchi, K. Ishimaru, and A. Ohno. Diel vertical migration of myctophid fishes (Family Myctophidae) in the transitional waters of the western North Pacific. *Fisheries Oceanography*, 8(2):115–127, 1999.

A M Values Function

```
library(tidyverse)
library(HDInterval)
library(truncnorm)
        ,
M_val <- function(d13C, d13C_sd,
                  # d13C_otolith value and SD
                  Year,
                  # Year of capture
                  reps,
                  # Number of repetitions when sampling from distributions
                  DIC_surf, DIC_surf_sd,
                  # d13C_DIC value and SD from capture location
                  DIC_min, DIC_max,
                  # Global d13C_DIC min and max
                  suess, suess_sd,
                  # Post-1970 Suess effect and SD from capture location
                  suess_min, suess_max,
                  # Global Suess effect min and max
                  suess_1970, suess_1970_sd,
                  # Pre-1970 Suess effect and SD
                  phyto, phyto_sd,
                  # d13C_phyto and SD from capture location
                  phyto_min, phyto_max,
                  # Global d13C_phyto min and max
                  phyto_suess, phyto_suess_sd,
                  # Suess effect for phytoplankton and SD
                  troph, troph_se,
                  # Trophic level and SE
                  troph_min, troph_max,
                  # Min and max trophic level for fishes
                  enrich, enrich_se,
                  # Trophic enrichment of d13C and SD
                  e_value){ # e (fractiontion) term

  # Calculate distributions of component values with set.seeds to ensure reproducibility
  set.seed(d13C)
  dist_d13C <- rnorm(reps, d13C, d13C_sd)
  set.seed(DIC_surf)
  dist_DIC_surf <- rtruncnorm(reps, DIC_min, DIC_max, DIC_surf, DIC_surf_sd)
  set.seed(suess)
  dist_suess <- rtruncnorm(reps, suess_min, suess_max, suess, suess_sd)
  set.seed(suess_1970)
  dist_suess_1970 <- rtruncnorm(reps, suess_min, suess_max, suess_1970, suess_1970_sd)
  set.seed(phyto)
  dist_phyto <- rtruncnorm(reps, phyto_min, phyto_max, phyto, phyto_sd)
  set.seed(phyto_suess)
  dist_phyto_suess <- rtruncnorm(reps, suess_min, suess_max, phyto_suess, phyto_suess_sd)
  set.seed(troph)
  dist_troph <- rtruncnorm(reps, troph_min, troph_max, troph, troph_se)
  set.seed(enrich)
  dist_enrich <- rnorm(reps, enrich, enrich_se)
  set.seed(Sys.time())
```

```
  # Calculate d13C_DIC, correcting for the Suess effect
  dist_DIC <- if(Year < 1970){
    dist_DIC_surf-(dist_suess_1970*((1990-Year)/10))
  } else if(Year < 1990){
    dist_DIC_surf-(dist_suess*((1990-Year)/10))
  } else {
    dist_DIC_surf+(dist_suess*((1990-Year)/10))
  }

  # Calculate d13C_Phyto, correcting for the Suess effect
  dist_phyto_corr <- if(Year < 1970){
    dist_phyto-(dist_phyto_suess*((2001-Year)/10))
  } else if(Year < 2001){
    dist_phyto-(dist_phyto_suess*((2001-Year)/10))
  } else if(Year > 2010){
    dist_phyto+(dist_phyto_suess*((2010-Year)/10))
  } else {
    dist_phyto
  }

  # Calculate d13C_diet
  dist_diet <- dist_phyto_corr + (dist_troph - 1) * dist_enrich

  # Calculate M
  dist_M <- (dist_d13C - dist_DIC) / (dist_diet - dist_DIC) + e_value

  # Get maximum density value for M
  max_dens <- which.max(density(dist_M)$y)
  M <- density(dist_M)$x[max_dens]

  # Get minimum, maximum and sd for M distribution
  min_M <- min(dist_M)
  max_M <- max(dist_M)
  sd_M <- sd(dist_M)

  # Combine results
  result <- data.frame(M, sd_M, min_M, max_M)
  return(result)
}
```

```
# Read in data

setwd("~/PhD/GitHub/mytophid-ears")
load("Functions/M_Val.Rdata")
myct <- read.csv("Data/Myctophids_Master.csv")

with(myct[2,], # Fish number two in master data set
     M_Val(d13C, 0.02,
           # SD from isotope lab
           Year.x, 10000,
           DIC, 0.202, 0, 3,
           # From Tagliabue & Bopp, 2007
           Suess, 0.202, -0.28, 0,
           # From Tagliabue & Bopp, 2007. SD same as for DIC
```

```
            -0.07, 0.202,
            # From Tagliabue & Bopp, 2007. SD same as for DIC
            Phyto, Phyto_sd, -31, -16.5,
            # From Magozzi et al. 2017. Based on values for Longhurst provinces
            -0.17, 0.202,
            # From Clive - per comms. SD same as for DIC
            UseTroph, UseTrophSe, 2, 5,
            # From FishBase
            0.8, 1.1,
            # From DeNiro & Epstein 1978
            0)) # From Solomon et al. 2006
```

```
##          M       sd_M     min_M     max_M
## 1 0.258657 0.02391067 0.1944767 0.3897002
```

- M = value at maximum density of distribution of M values.
- sd_M = standard deviation of M distribution.
- min_M = minimum value of M distribution.
- max_M = maximum value of M distribution.

B Temperature Function

```
library(tidyverse)
library(HDInterval)
library(truncnorm)
        ,
Temp_Vals <- function(d18O, d18O_sd,
                              # d18O_otolith values and SD
                              d18O_water, d18O_water_sd,
                              # d18O_SW values and SD
                              d18O_water_min, d18O_water_max,
                              # Global min and max for d18O_SW
                              reps){
                              # Number of repetitions when sampling from distributions

  # Calculate distributions of component values with set.seeds to ensure reproducibility
  set.seed(d18O)
  dist_d18O <- rnorm(reps, d18O, d18O_sd)
  set.seed(d18O_water)
  dist_d18O_water <- rtruncnorm(reps, d18O_water_min, d18O_water_max, d18O_water,
                                d18O_water_sd)
  # Set parameter values from Hoie et al. 2004
  set.seed(3.9)
  dist_param_1 <- rnorm(reps, 3.90, 0.24)
  set.seed(-0.20)
  dist_param_2 <- rnorm(reps, -0.20, 0.019)

  # Calculate temperature
  dist_d18 <- dist_d18O - dist_d18O_water
  dist_temp <- (dist_d18 - dist_param_1)/dist_param_2

  # Get maximum density of temperature
  max_dens <- which.max(density(dist_temp)$y)
  temp <- density(dist_temp)$x[max_dens]

  # Get minimum, maximum and sd of temperature
  min_temp <- min(dist_temp)
  max_temp <- max(dist_temp)
  sd_temp <- sd(dist_temp)

  # Return results
  result <- data.frame(temp, sd_temp, min_temp, max_temp)
  return(result)
}
```

```
# Read in and tidy data
setwd("~/PhD/GitHub/mytophid-ears")
myct <- read.csv("Data/Myctophids_Master.csv")
myct <- filter(myct, d13C != "NA")
d18O_sd <- sd(myct$D18O_vals)
d18O_min <- min(myct$D18O_vals)
d18O_max <- max(myct$D18O_vals)

with(myct[3,], # Fish number three in master data set
     Temp_Vals(d18O, 0.02, # SD from isotope data
                       D18O_vals, d18O_sd, # SD from data
```

```
                      d18O_min, d18O_max, # Min-max from data
                      10000))
```

```
##        temp  sd_temp  min_temp max_temp
## 1 0.1037534 1.230554 -4.258677 5.742518
```

- temp = value at maximum density of distribution of temperature values.
- sd_temp = standard deviation of temperature distribution.
- min_temp = minimum value of temperature distribution.
- max_temp = maximum value of temperature distribution.

C Supplementary Analyses

There was no significant difference between maximum density estimates of M values between otolith samples that were milled and crushed ($F(1, 18) = 1.63$, $p = 0.218$) in *Protomyctophum bolini*, the only species for which otoliths were both crushed and milled. Across all species, with species as a random factor, maximum density estimates of M values were slightly lower for milled compared to crushed otoliths (estimate of effect of milling = -0.03112 $\pm$0.01519).

D Traceplots

D.1 Model 1 - Body Mass and Temperature

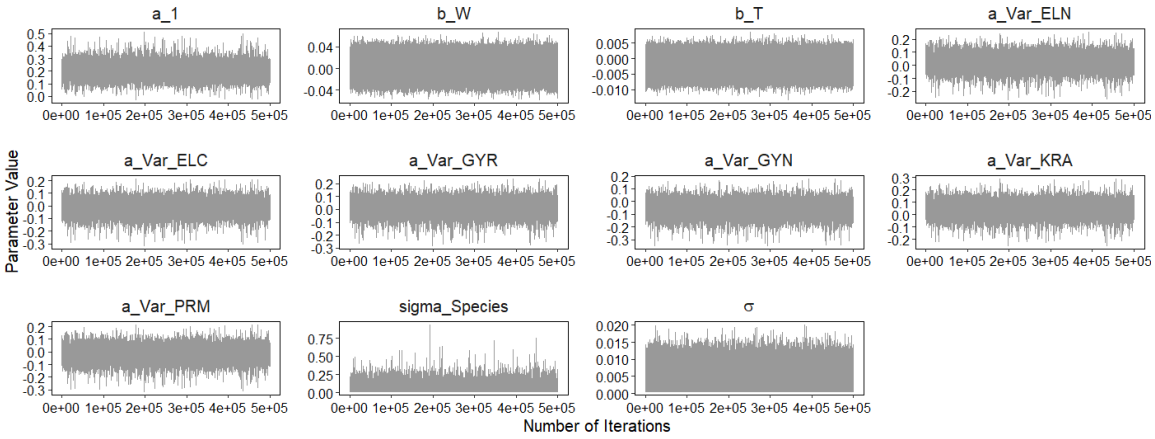

D.2 Model 2 - Temperature

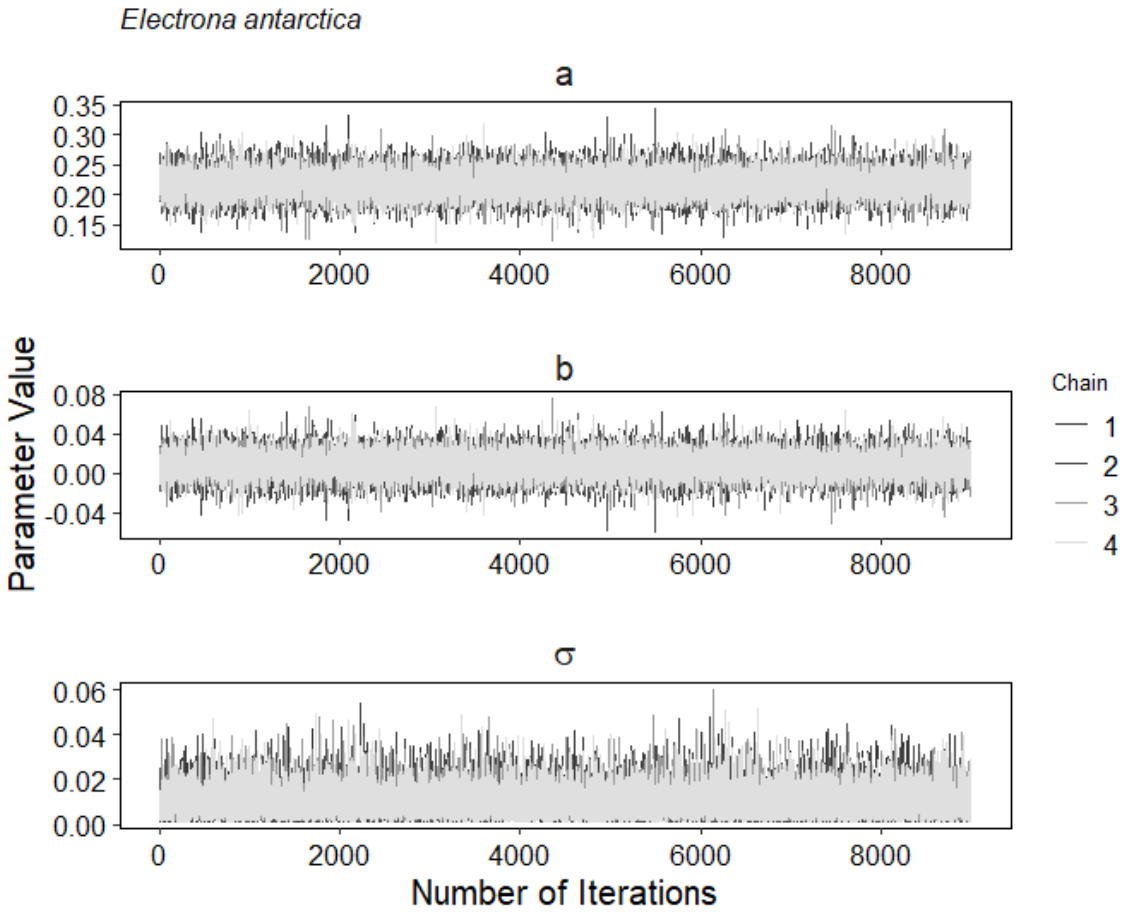

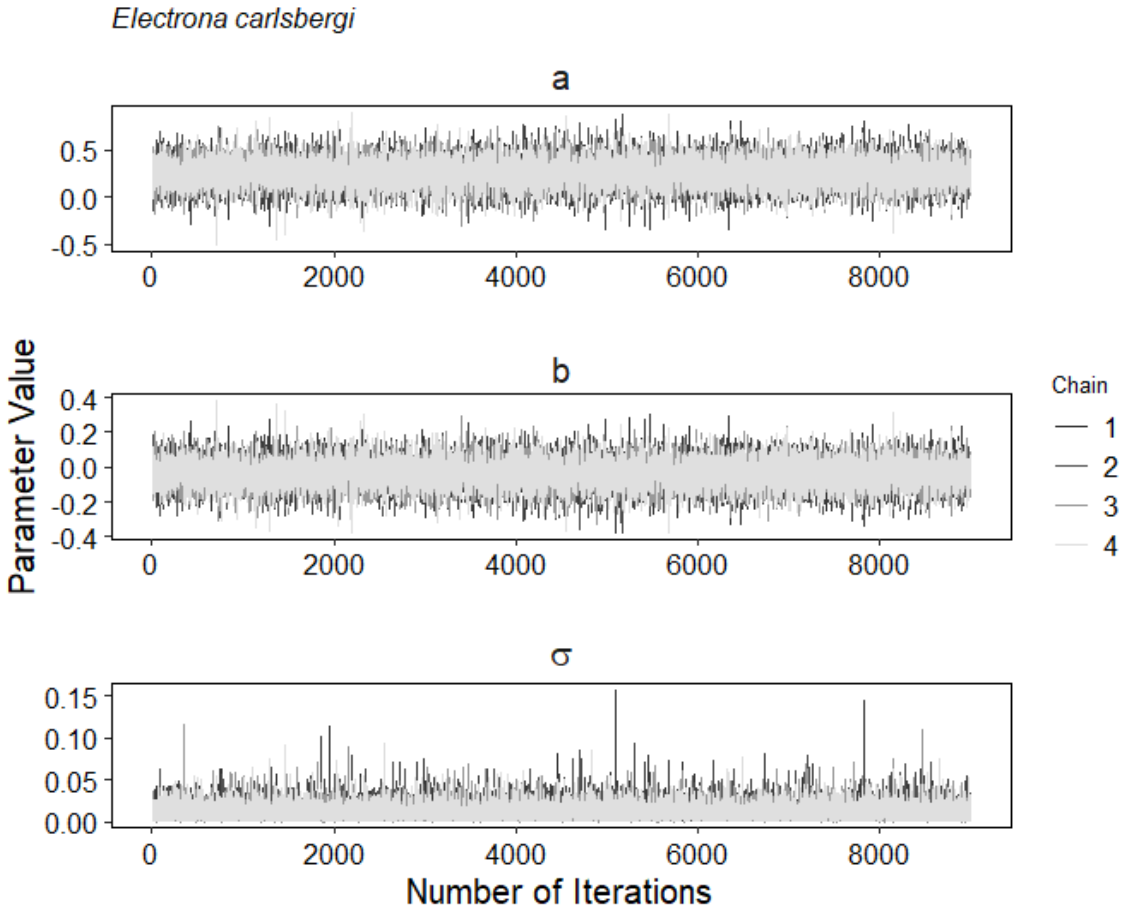
Electrona carlsbergi
a
b
σ
Parameter Value
Number of Iterations
Chain
1
2
3
4

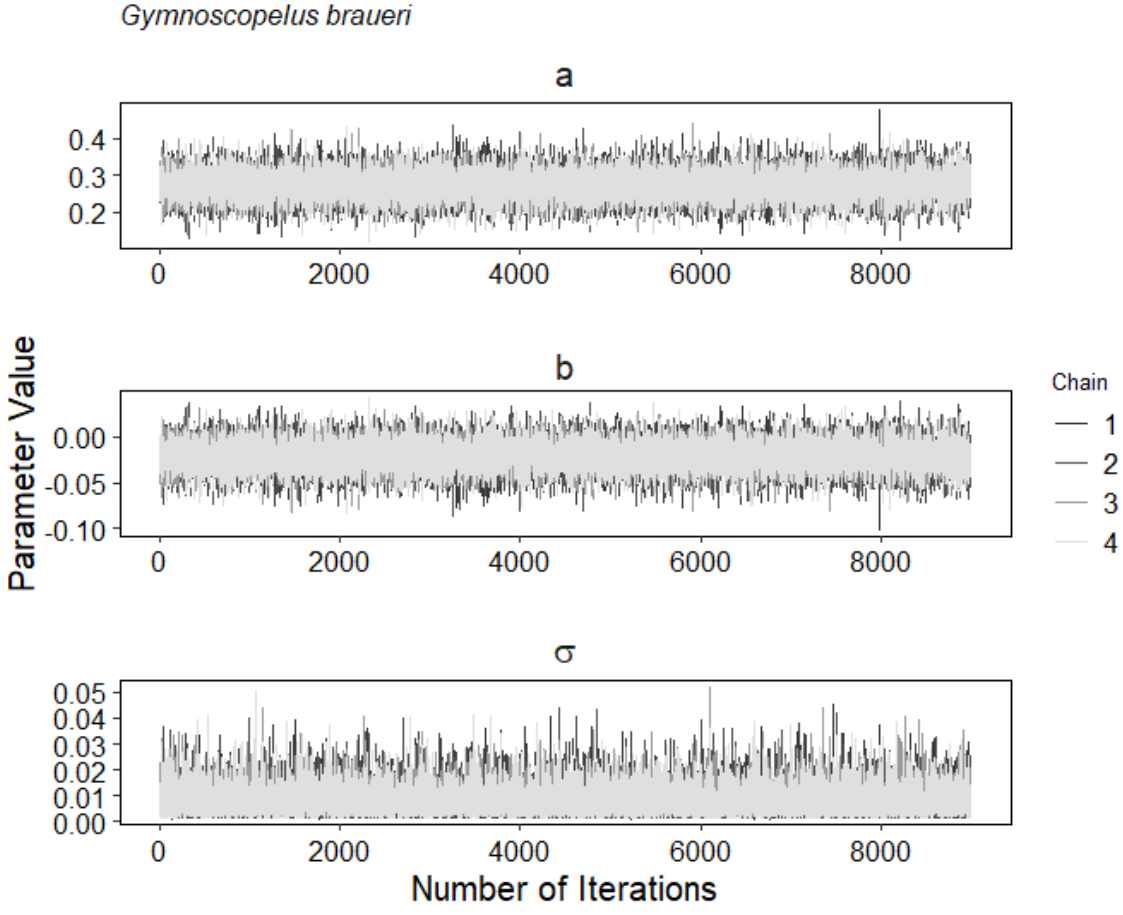
Gymnoscopelus braueri
a
b
σ
Parameter Value
Number of Iterations
Chain
1
2
3
4

Gymnoscopelus nicholsi

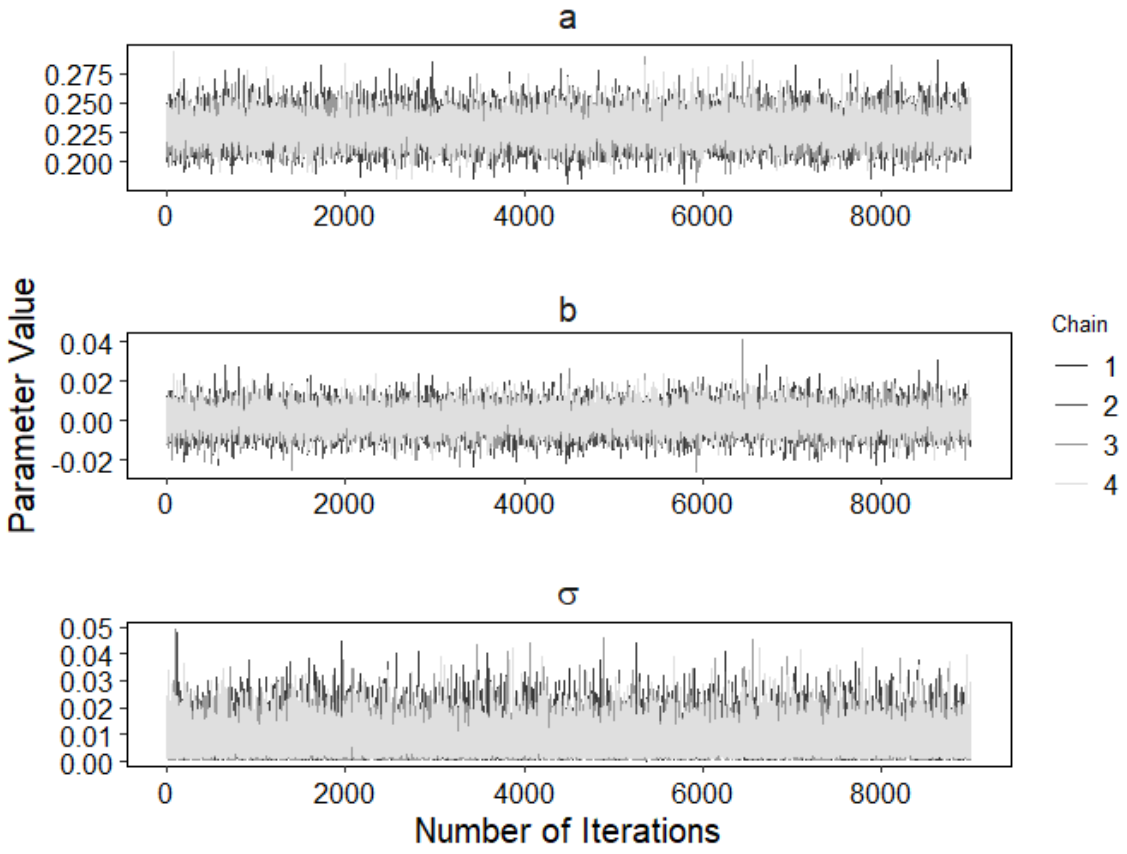

Krefftichthys anderssoni

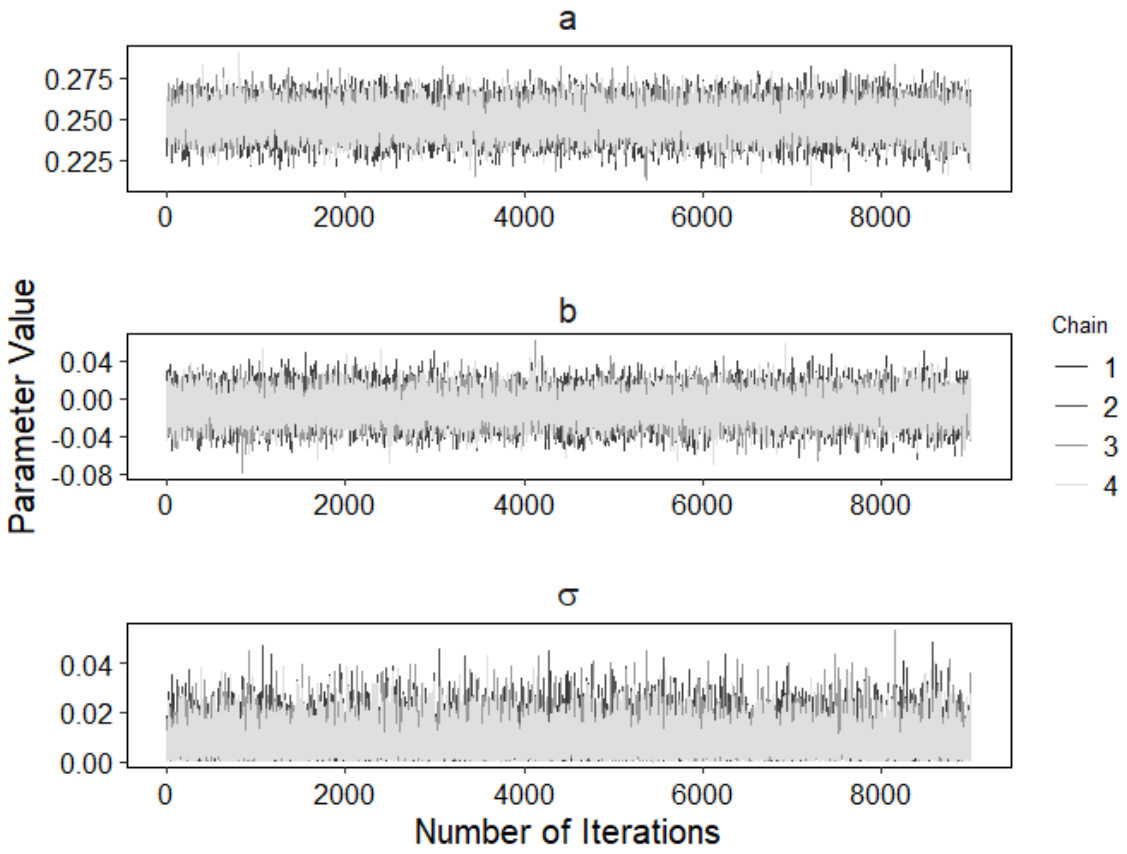

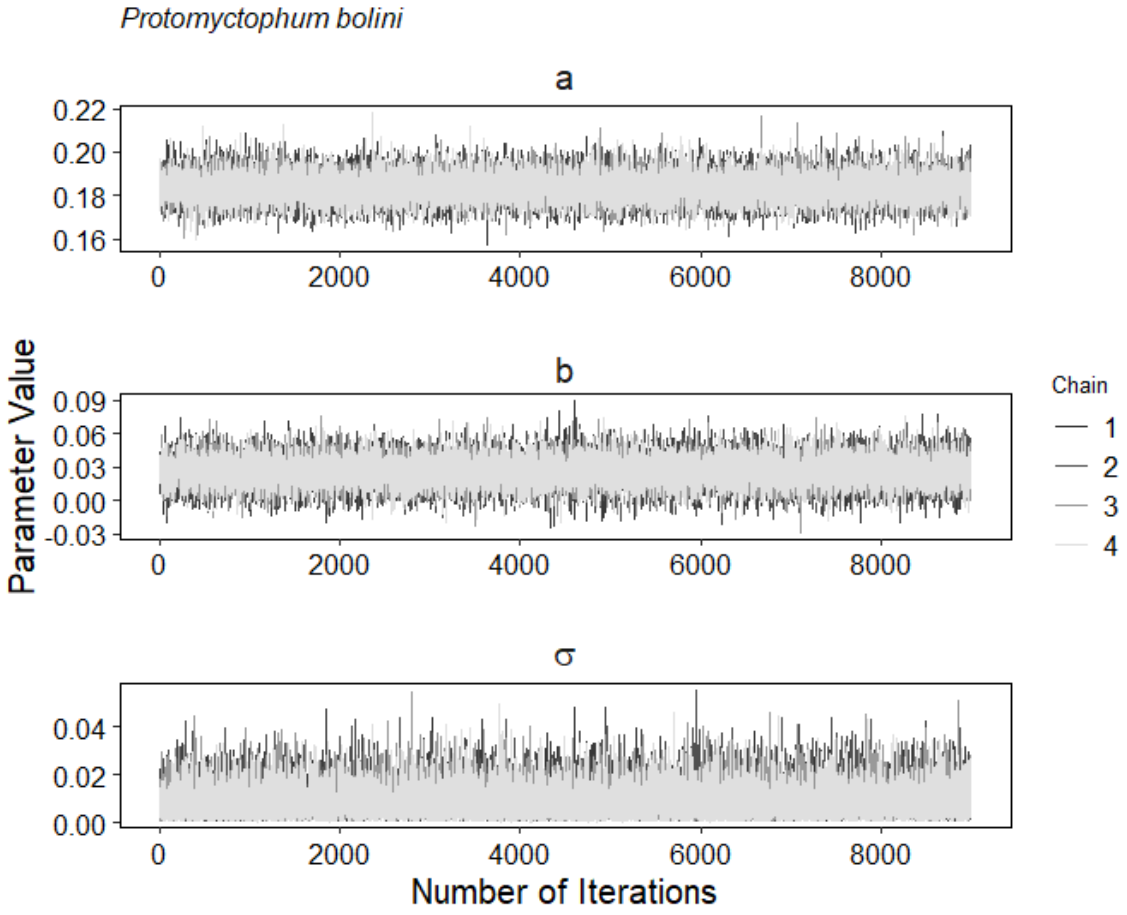
Protomyctophum bolini
a
0.22
0.20
0.18
0.16
0
2000
4000
6000
8000
b
0.09
0.06
0.03
0.00
-0.03
σ
0.04
0.02
0.00
Parameter Value
Number of Iterations
Chain
1
2
3
4

D.3 Model 3 - Body Mass

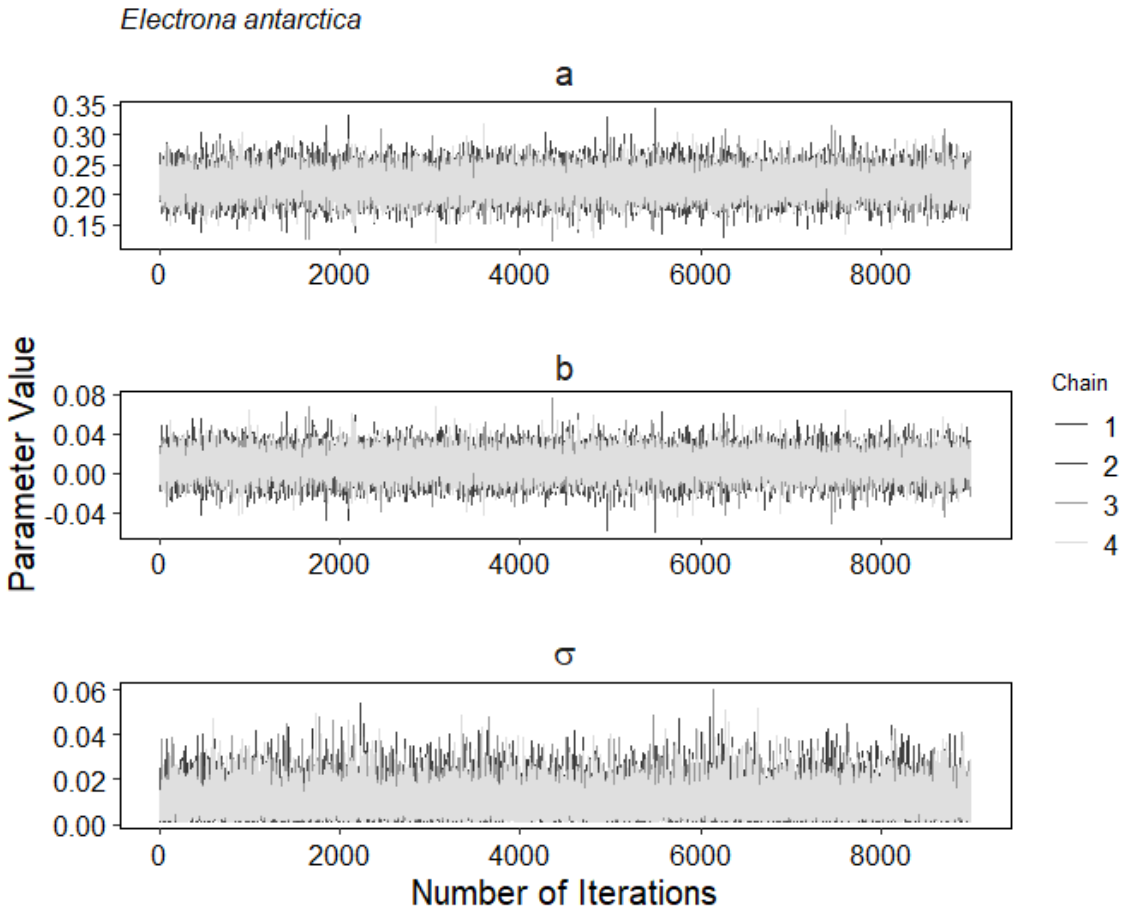

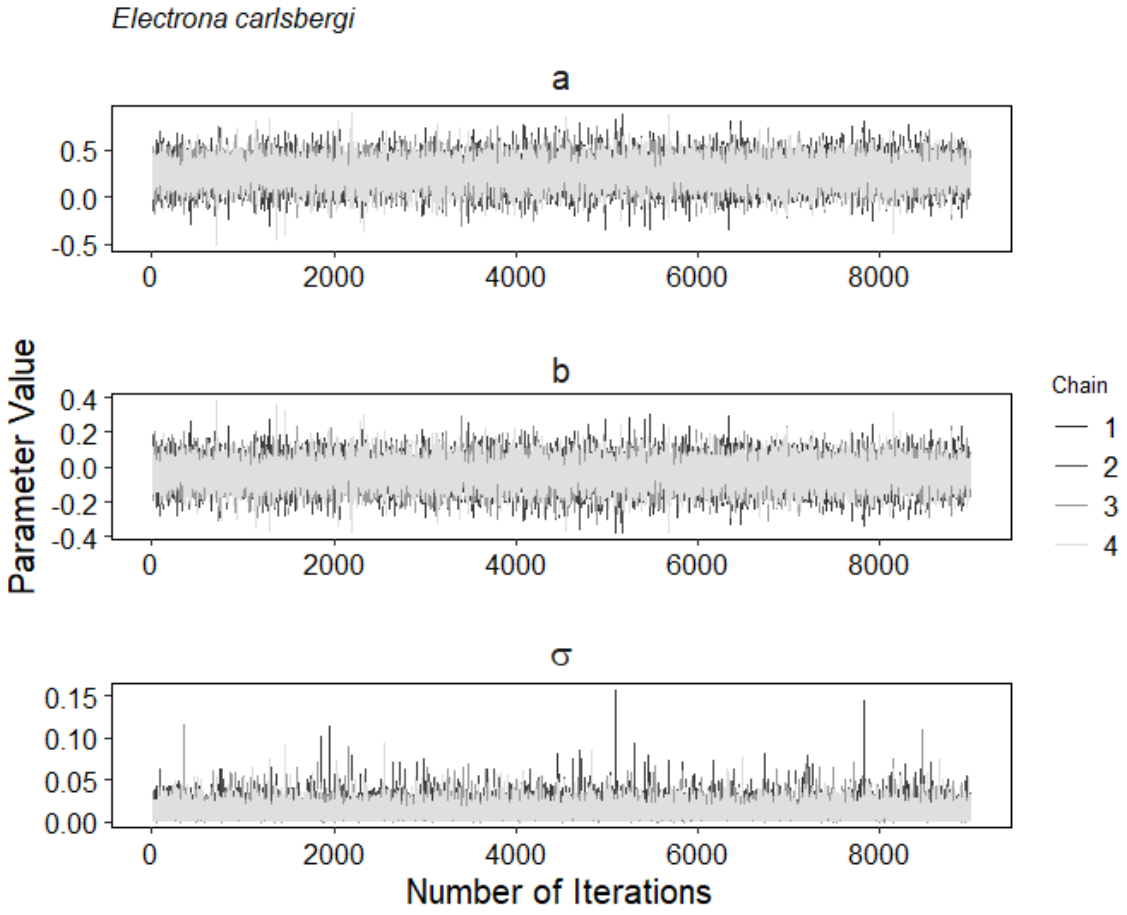
Electrona carlsbergi
a
b
σ
Parameter Value
Number of Iterations
Chain
1
2
3
4

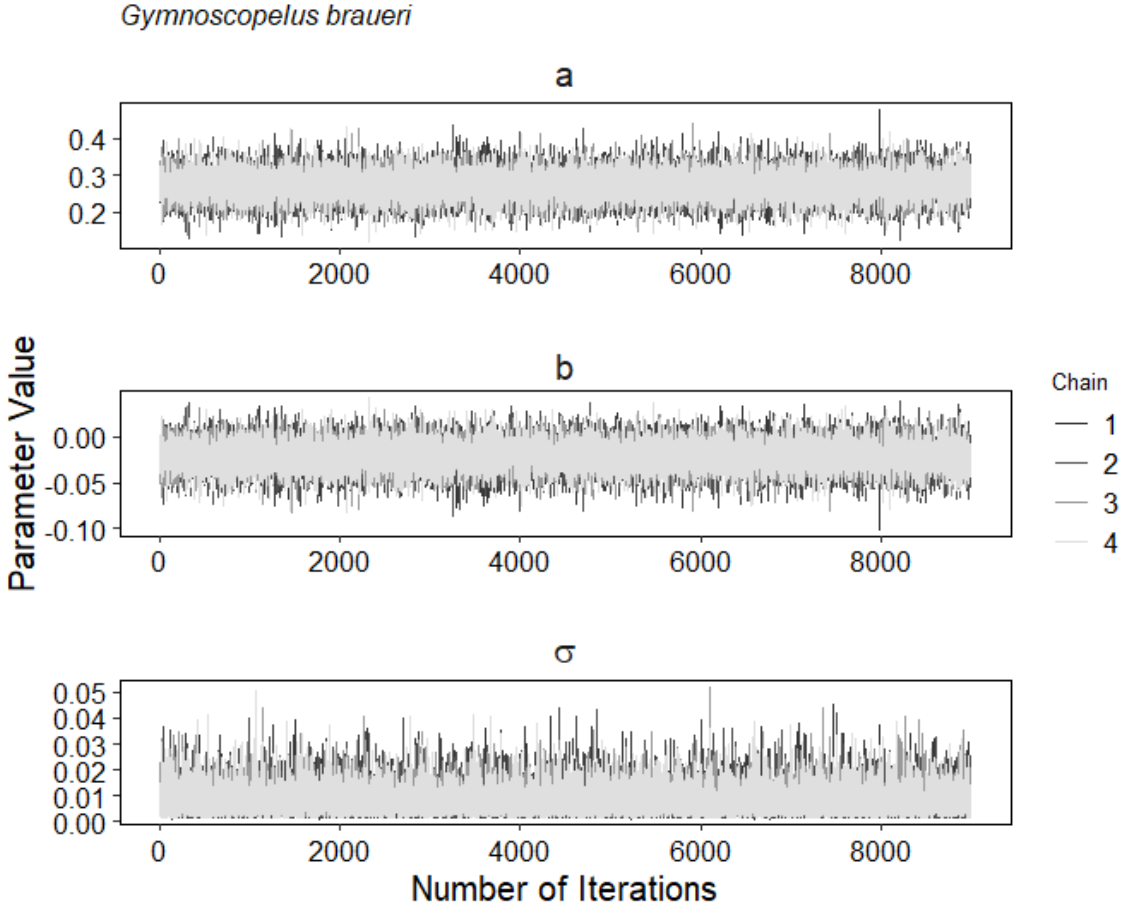
Gymnoscopelus braueri
a
b
σ
Parameter Value
Number of Iterations
Chain
1
2
3
4

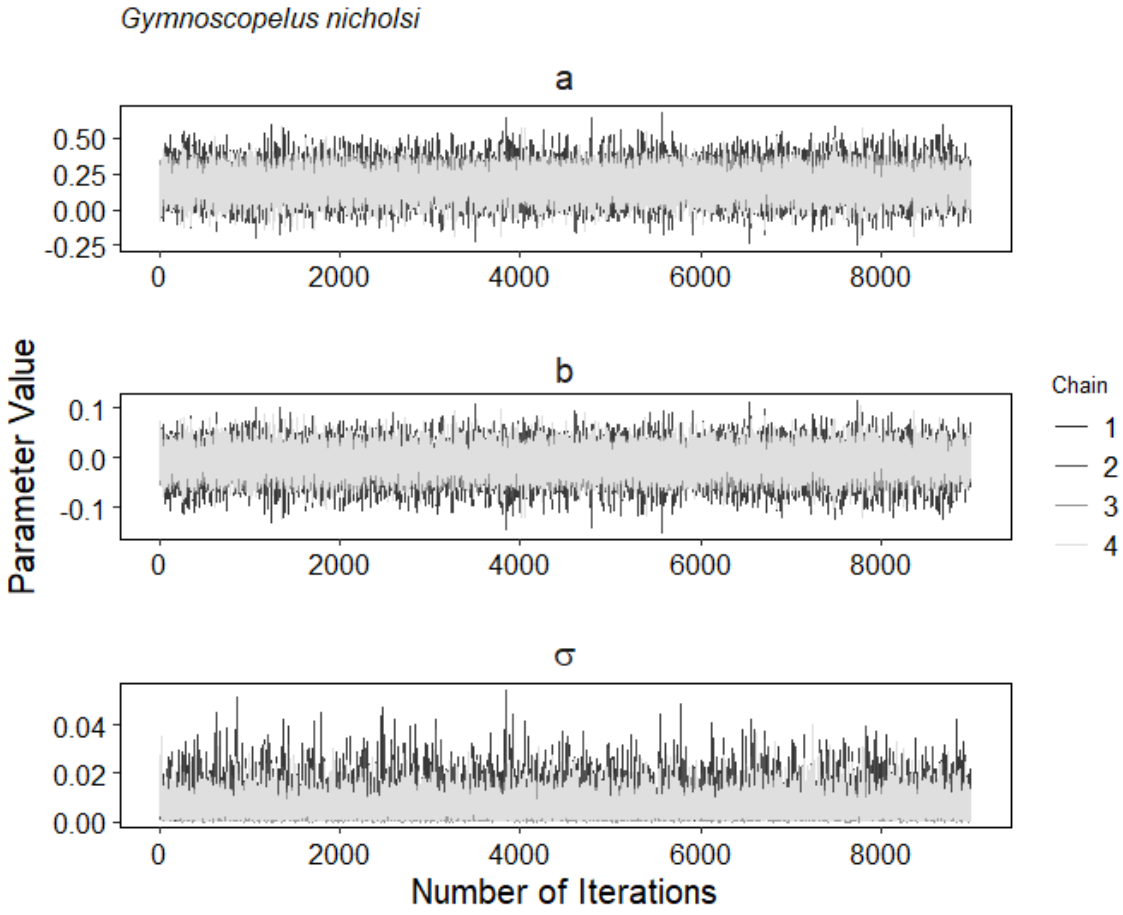
Gymnoscopelus nicholsi
a
0.50
0.25
0.00
-0.25
0
2000
4000
6000
8000
b
0.1
0.0
-0.1
σ
0.04
0.02
0.00
Parameter Value
Number of Iterations
Chain
1
2
3
4

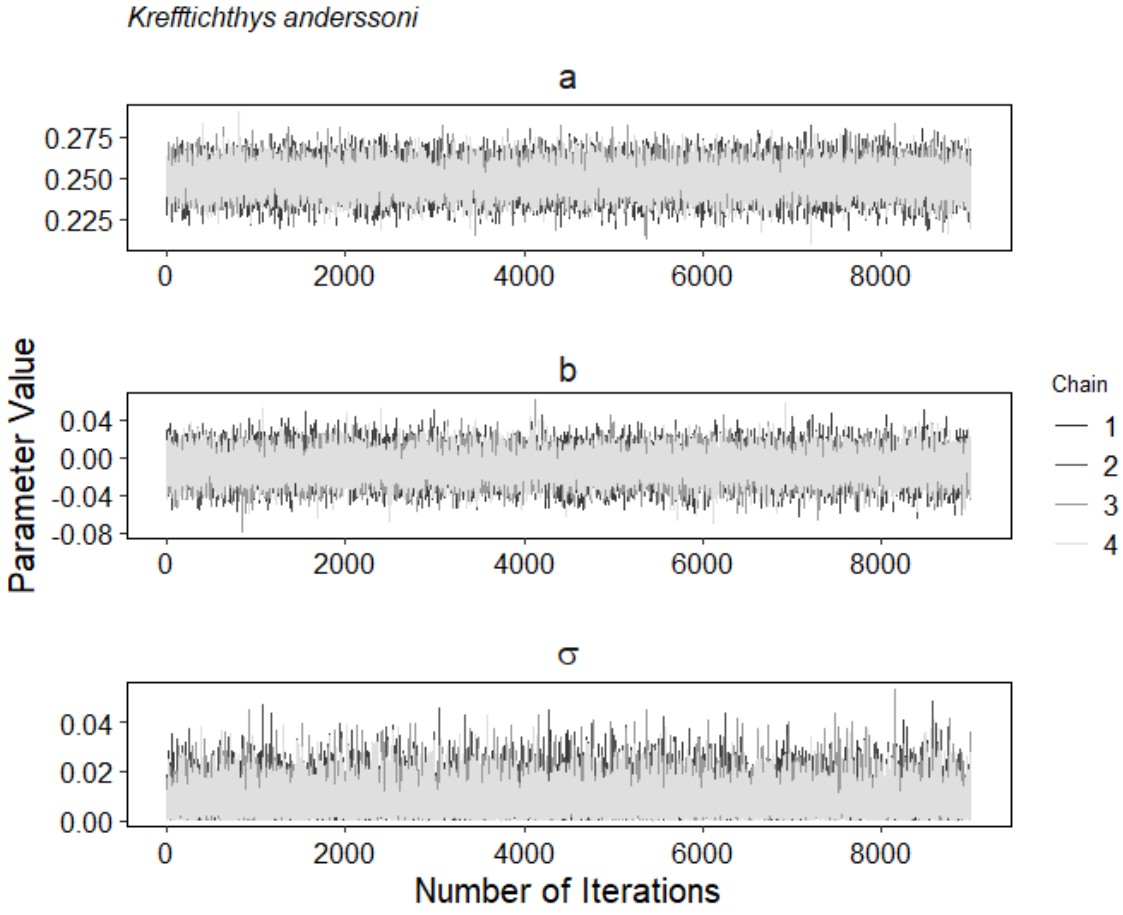
Krefftichthys anderssoni
a
0.275
0.250
0.225
0
2000
4000
6000
8000
b
0.04
0.00
-0.04
-0.08
σ
0.04
0.02
0.00
Parameter Value
Number of Iterations
Chain
1
2
3
4

Protomyctophum bolini

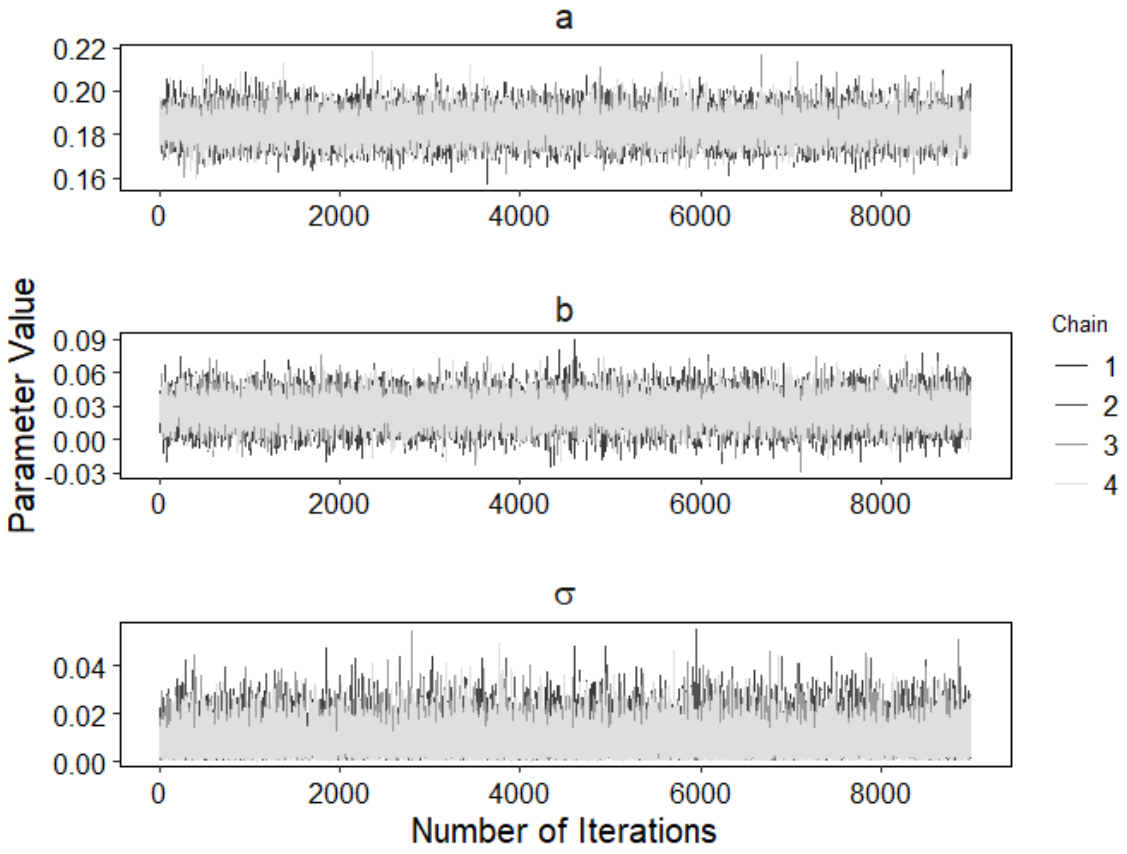

D.4 Model 4 - Resting Metabolic Rate

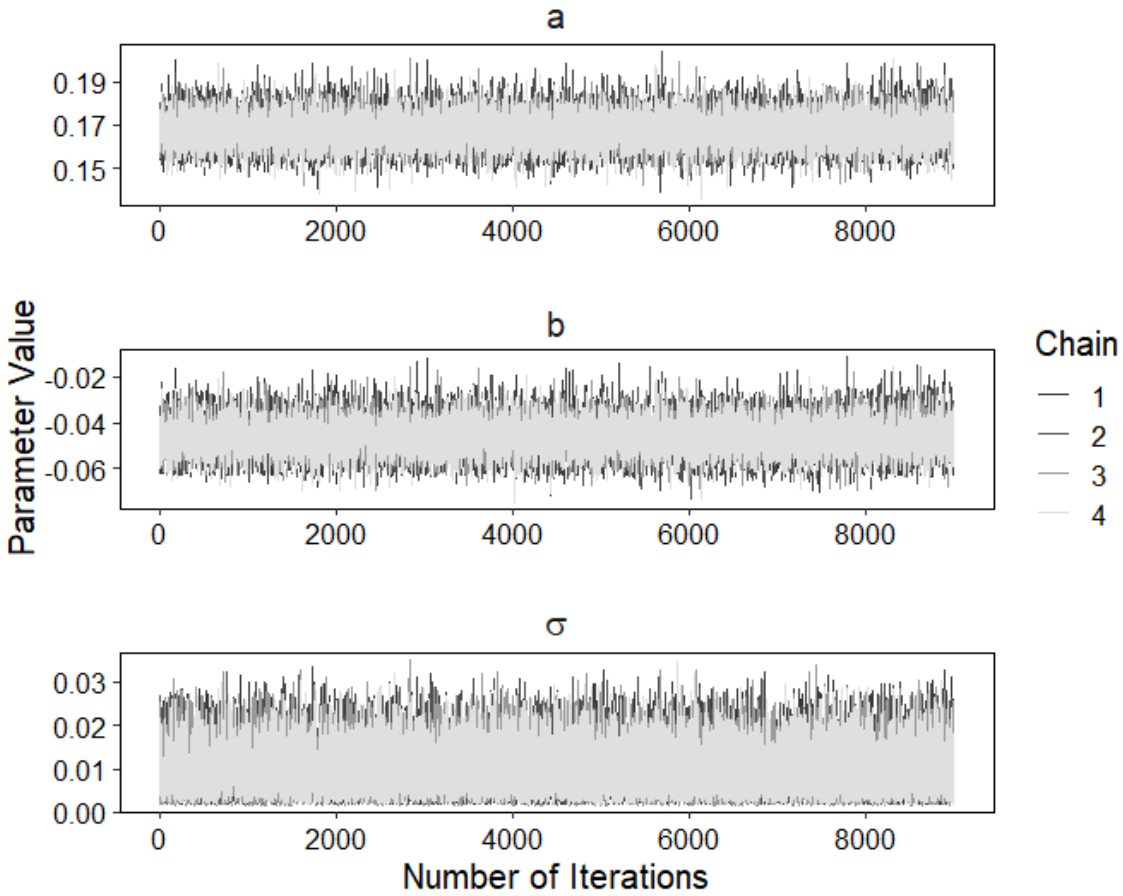

E Sensitivity Analysis for M Function

This sensitivity analysis was carried out on my main data set (section 7.2). The violin plots show the distribution of maximum density of M values for individuals from this dataset. Violins marked "baseline" have values set according to those used in this study (section 3.1.2).

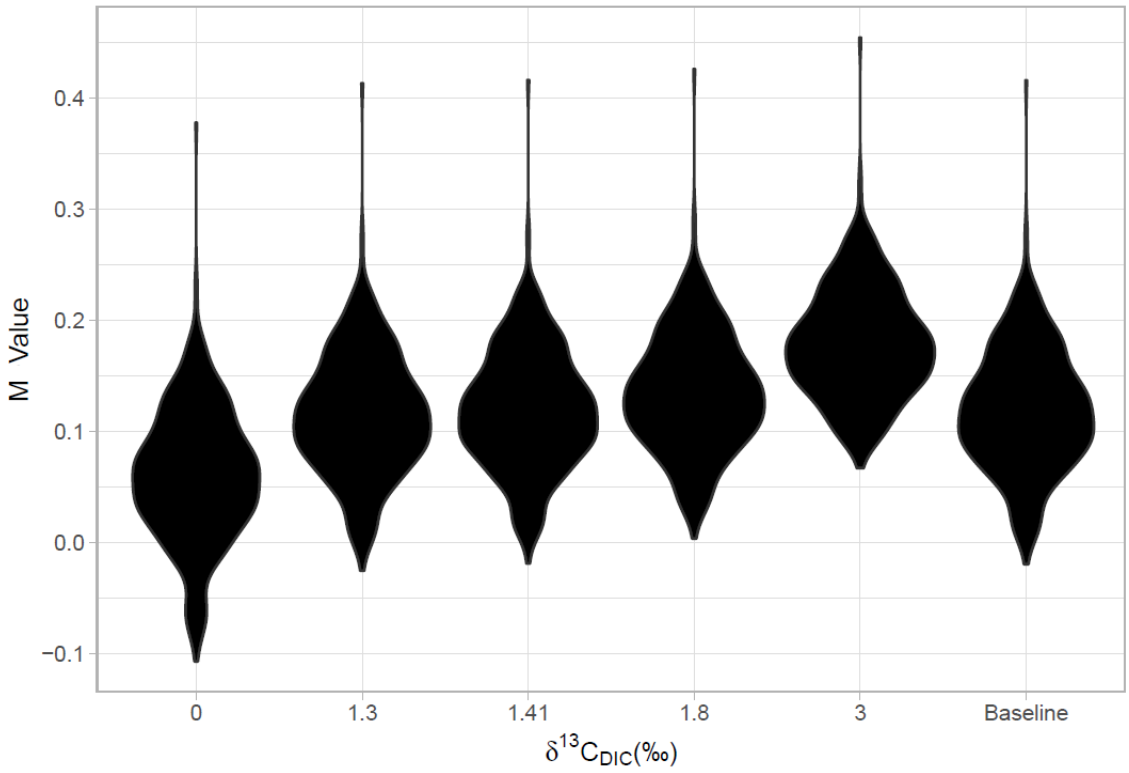

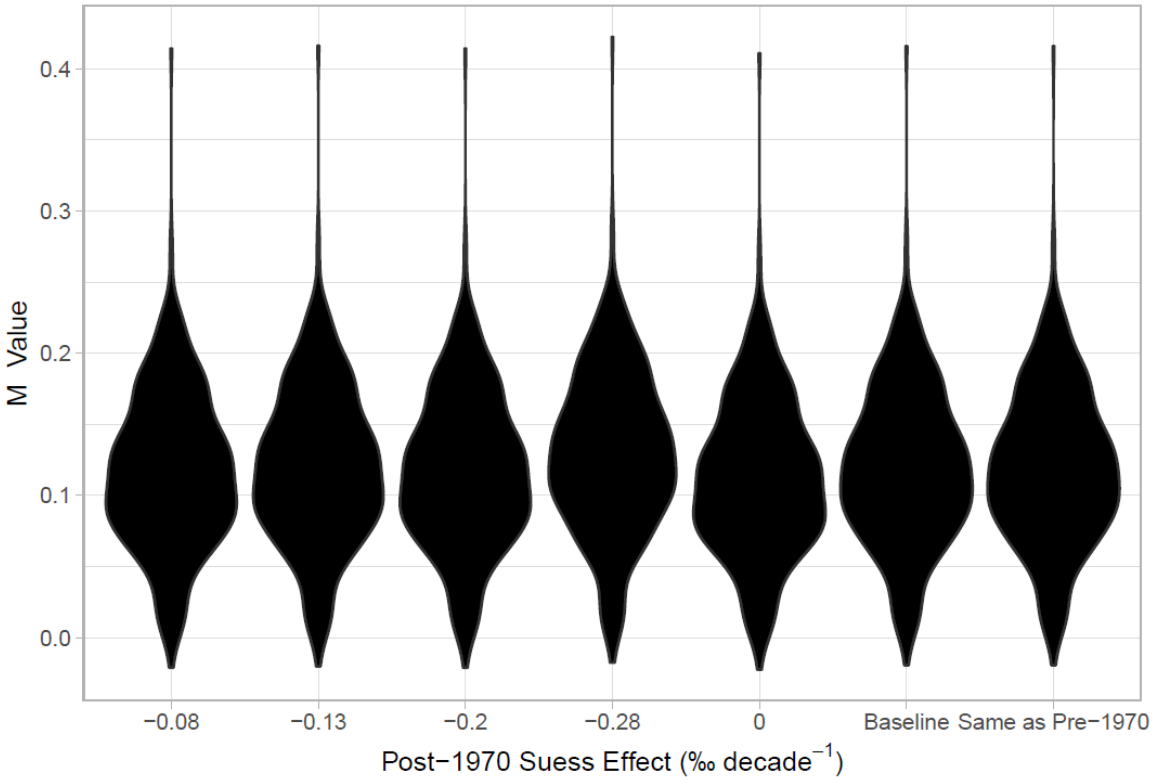
M Value
0.4
0.3
0.2
0.1
0.0
−0.08
−0.13
−0.2
−0.28
0
Baseline Same as Pre−1970
Post−1970 Suess Effect (‰ decade^{-1})

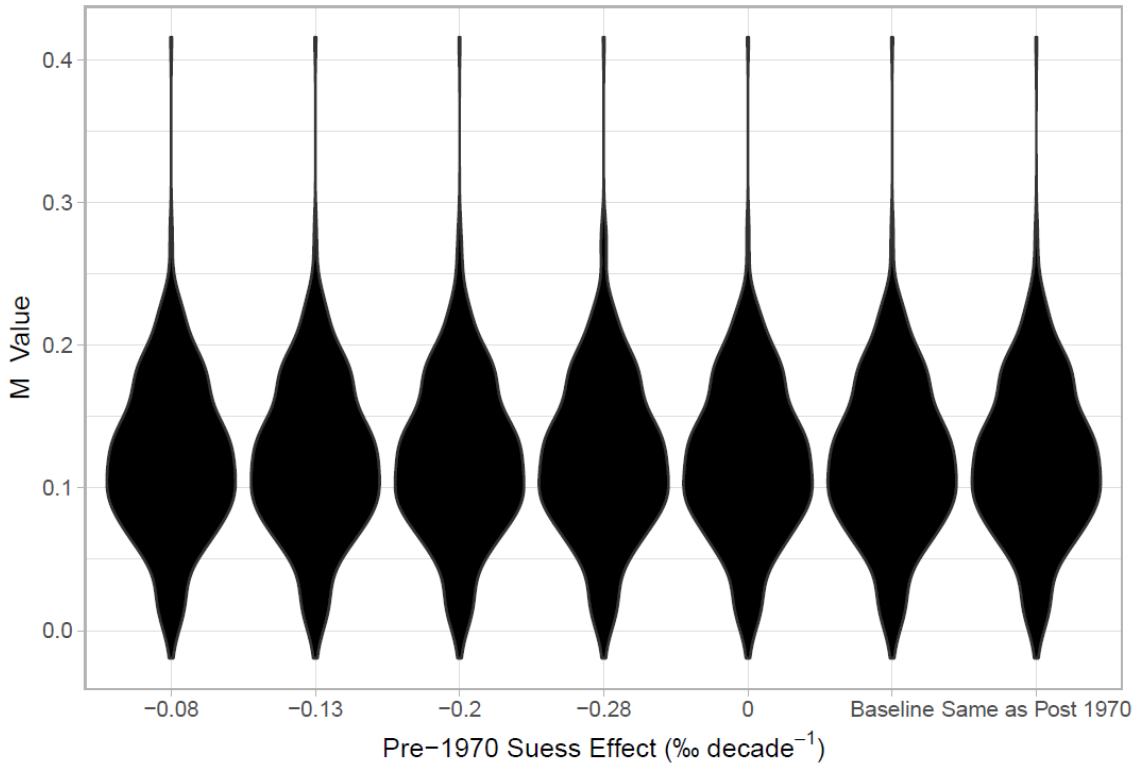
M Value
0.4
0.3
0.2
0.1
0.0
−0.08
−0.13
−0.2
−0.28
0
Baseline Same as Post 1970
Pre−1970 Suess Effect (‰ decade^{-1})

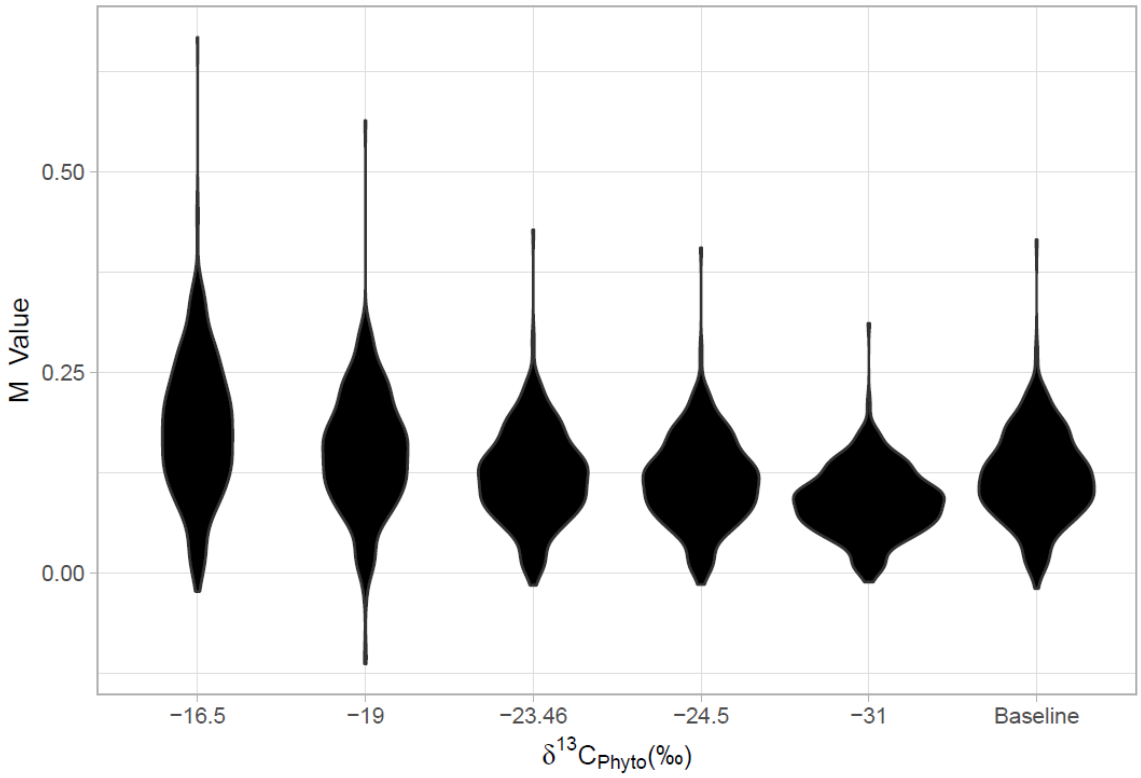
M Value
0.50
0.25
0.00
−16.5
−19
−23.46
−24.5
−31
Baseline
δ13CPhyto(‰)

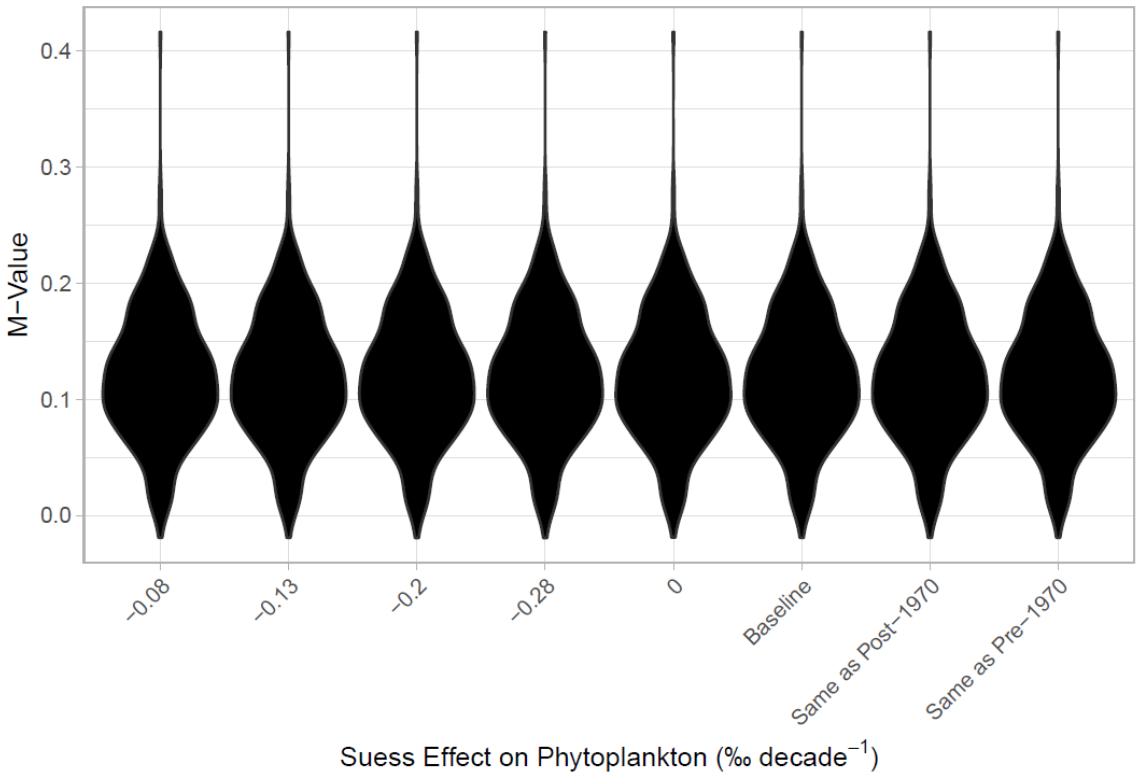
M−Value
0.4
0.3
0.2
0.1
0.0
−0.08
−0.13
−0.2
−0.28
0
Baseline
Same as Post−1970
Same as Pre−1970
Suess Effect on Phytoplankton (‰ decade−1)

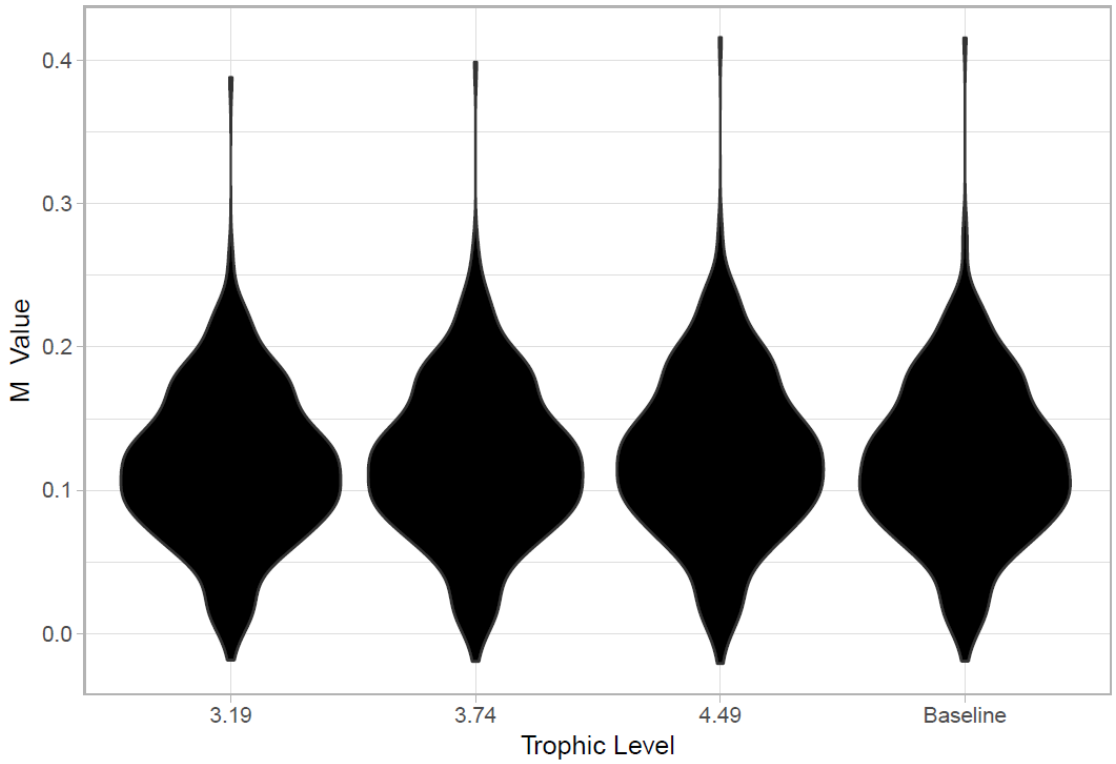
0.4
0.3
0.2
0.1
0.0
M Value
3.19
3.74
4.49
Baseline
Trophic Level

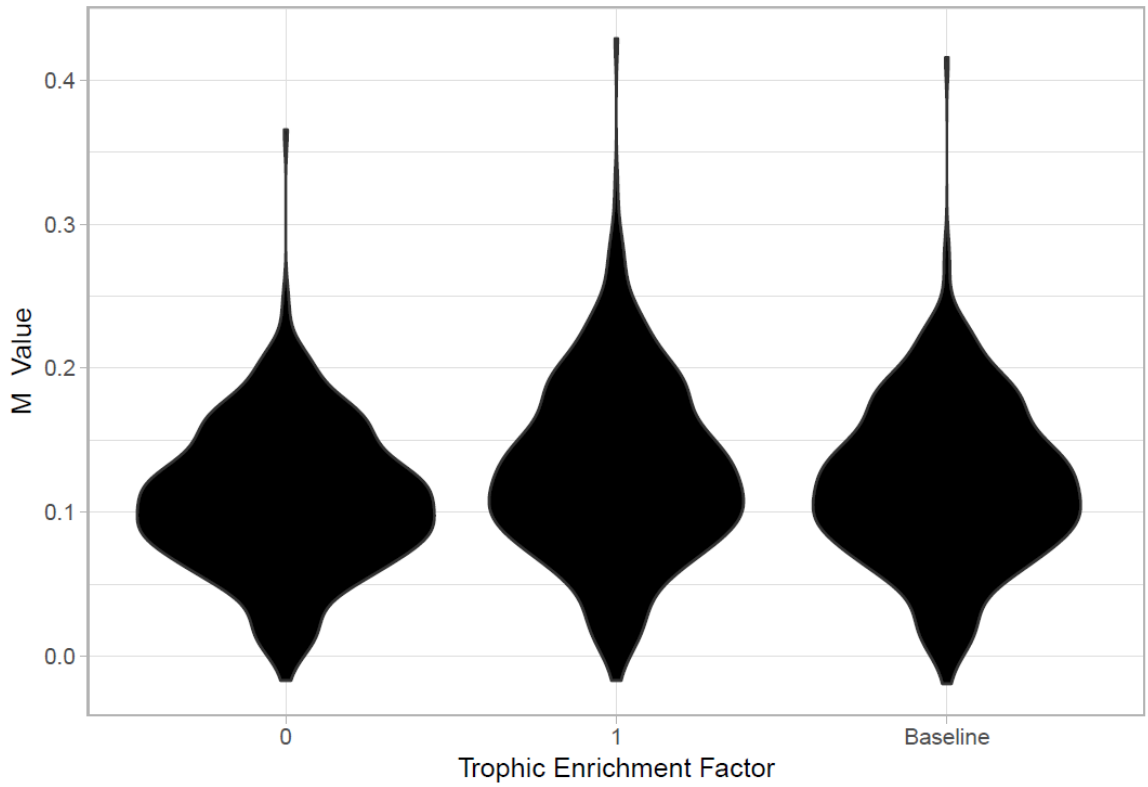
0.4
0.3
0.2
0.1
0.0
M Value
0
1
Baseline
Trophic Enrichment Factor

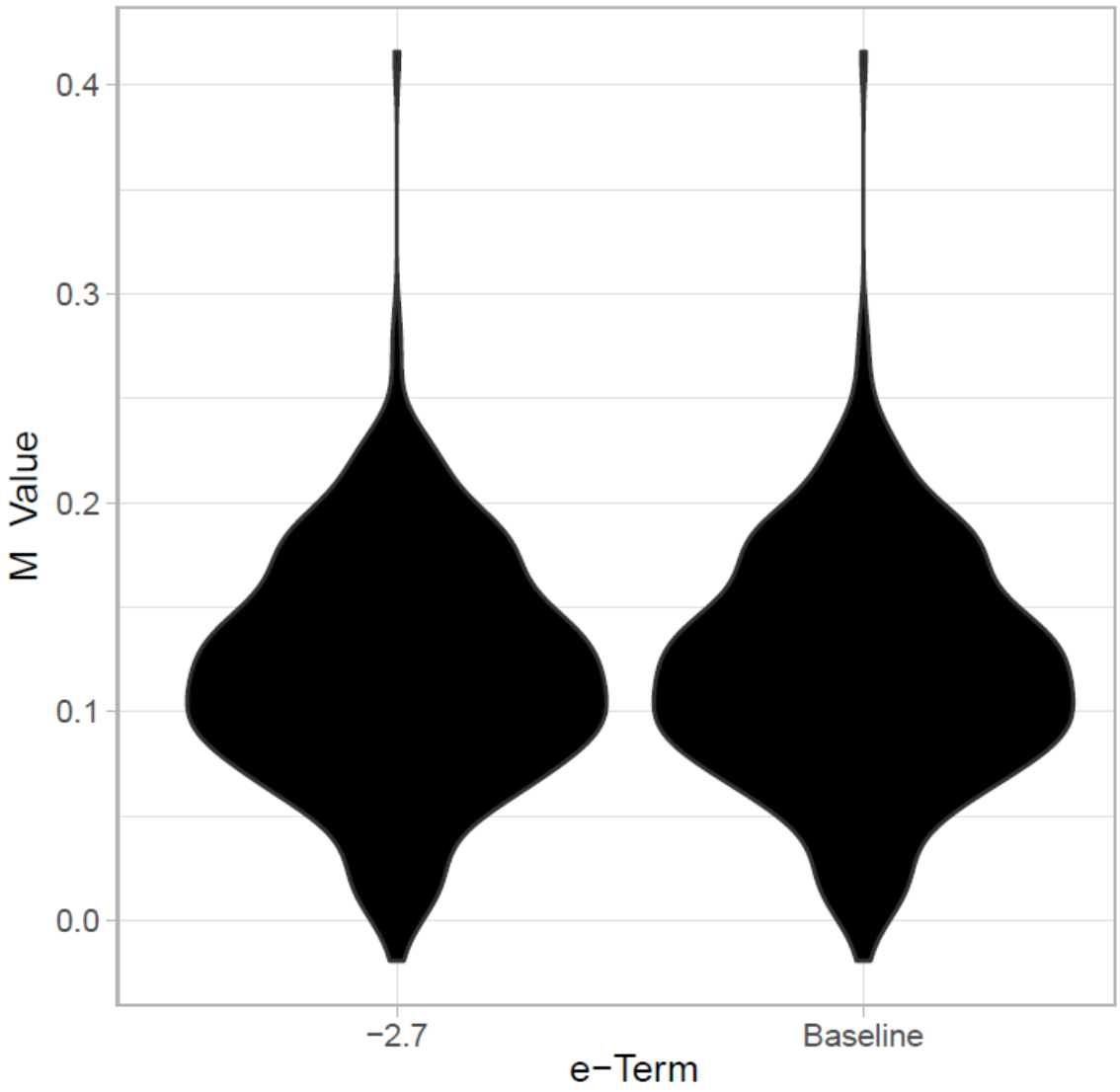
0.4
0.3
0.2
0.1
0.0
M Value
−2.7
Baseline
e−Term